UNIVERSITÀ DEGLI STUDI DI MILANO

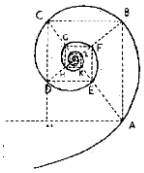

DOTTORATO IN MEDICINA MOLECOLARE E TRASLAZIONALE

CICLO XXIX

Anno Accademico 2015/2016

TESI DI DOTTORATO DI RICERCA

MED/04

TRANSCRIPTOMIC ANALYSIS IN SEPTIC SHOCK PATIENTS

Dottorando : Daniele BRAGA

Matricola N° R10729

TUTORE: Dott.ssa Cristina BARLASSINA

DIRETTORE DEL DOTTORATO: Prof. Mario CLERICI

SOMMARIO

Introduzione

Lo shock settico, altrimenti definito shock distributivo, è una complicanza della sepsi, caratterizzato da ipotensione marcata, con conseguente anomala distribuzione di sangue a vasi, organi e tessuti. Le alterazioni emodinamiche, cellulari e metaboliche descritte nei pazienti in shock settico portano ad una mortalità che è attualmente intorno al 40 %. I pazienti in shock settico sviluppano disfunzioni a più organi (MOF) ma i meccanismi molecolari che innescano il danno a livello dei tessuti sono ancora per la maggior parte sconosciuti e un trattamento specifico per lo shock settico non è ancora disponibile.

Scopo

Questo lavoro è parte del Progetto Europeo "ShockOmics", uno studio multicentrico prospettico osservazionale, il cui obiettivo è identificare con un approccio multiscala, biomarkers molecolari nello scompenso cardiaco acuto in pazienti in shock settico.

Lo scopo specifico del presente progetto di Ricerca è indagare le modificazioni indotte dallo shock settico sul profilo trascrizionale, utilizzando come sorgente di RNA le cellule del sangue. Questa indagine è svolta a più punti temporali a partire dall'ammissione del paziente all'unità di terapia intensiva (ICU).

Materiali e Metodi

I pazienti in shock settico sono stati reclutati nelle unità di terapia intensiva degli Ospedali Universitari di Ginevra e Bruxelles, partners del Progetto ShockOmics. I campioni di sangue sono stati raccolti all'ammissione del paziente alla ICU, che corrisponde alla fase acuta della malattia (T1), dopo

che il paziente ha ricevuto le terapie farmacologiche necessarie (T2) e allo stato stazionario (T3) che corrisponde al giorno 7 dal ricovero. L'RNA è stato estratto da sangue intero e i livelli di espressione di geni, RNA lunghi non codificanti e microRNA sono stati valutati con esperimenti di RNAseq. Abbiamo esplorato il dataset con l'analisi delle componenti principali (PCA) e il clustering gerarchico non supervisionato. Sono stati identificati geni e microRNA differenzialmente espressi. I processi biologici coinvolti nello shock sono stati studiati con un'analisi di ontologie geniche. I geni target di microRNA sono stati identificati con un metodo di predizione in silico.

Risultati

Abbiamo identificato due profili di espressione genica che corrispondono alla condizione acuta dello shock e allo stato stazionario. Confrontando la fase acuta dello shock (giorno 1) con la condizione di stato stazionario (giorno 7), abbiamo osservato nei pazienti al giorno 7 la downregolazione di pathways della risposta immunitaria innata (recettori Toll-like e lectine di tipo C) e dell'infiammazione acuta (recettori delle interleukine di tipo 1 e allarmine) e l'upregolazione in questi pazienti di geni della risposta immune adattativa relativi all'attivazione di linfociti T e B. Abbiamo osservato una regolazione trascrizionale anche per geni con funzione antimicrobica, attività proteasica, geni coinvolti nel metabolismo dei carboidrati, nei pathways infiammatori lipidici, nel trasporto di vescicole e nella sintesi proteica. miR-125a-5p e miR-150-5p, per i quali è stato predetto un ruolo regolatorio del pathway delle MAP chinasi, e miR-193a-3p sono stati identificati come differenzialmente espressi tra la condizione acuta e lo stato stazionario.

Conclusioni

Abbiamo osservato una significativa modulazione trascrizionale di più classi di geni coinvolti nella risposta di difesa ai patogeni, nel sistema immunitario, nell'infiammazione e nel metabolismo. Questi risultati suggeriscono che nello shock settico viene indotta una rilevante modificazione del profilo trascrizionale nelle cellule del sangue conseguente alle alterazioni emodinamiche presenti nella condizione di shock e all'azione dei patogeni. Il profilo trascrizionale dei pazienti in shock circolatorio ha mostrato variabilità tra pazienti e ciò riflette la complessità della condizione di shock e della risposta individuale al trattamento. La combinazione dei dati clinici e del profilo di espressione genica potrebbe essere utile per identificare specifiche firme molecolari utili nella classificazione dei pazienti in shock settico.

ABSTRACT

Introduction

Septic shock, also defined as distributive shock, is a complication of sepsis, characterized by pronounced hypotension, followed by anomalous distribution of blood at vessels, organs and tissues. The hemodynamic, cellular and metabolic alterations described in septic shock patients lead to a mortality that is at present around 40%. Septic shock patients develop dysfunctions or failure to multiple organs (MOF) but the molecular mechanisms triggering tissue injury remain largely undetermined and a specific treatment for septic shock is still not available.

Aim

This work is part of the European Project ShockOmics, a multicentric, prospective, observational study, whose aim is to identify with a multiscale approach, molecular biomarkers in septic shock patients who develop acute heart failure. The specific aim of the present Research project is to investigate the modifications induced by septic shock on transcriptional profile, using blood cells as RNA source. This investigation is performed at different timepoints starting from admission of the patient to the intensive care unit (ICU).

Materials and Methods

Septic shock patients were recruited in the ICUs of Geneva and Bruxelles University Hospitals, that are Partners of ShockOmics Project. Blood samples were collected in the acute phase of the disease at ICU admission (T1), after the appropriate pharmacological intervention (T2) and at steady state on day 7 of the ICU stay (T3). RNA was extracted from whole blood and RNA sequencing was used to evaluate the expression level of genes,

long non coding RNAs and microRNAs. We explored the dataset using PCA and unsupervised hierarchical clustering and we identified differentially expressed genes and microRNAs across conditions. Gene Ontology analysis was used to identify relevant biological processes involved in shock. We identified microRNA regulatory targets with an in silico target prediction.

Results

We identified two main gene expression profiles corresponding to the acute phase of shock and to the condition of steady state. Between the acute phase of shock (day 1) and the steady state condition (day 7) we observed in patients at day 7 a downregulation of pathways of the innate immune response (Toll-like receptor and C-type lectin receptors pathways) and of acute inflammation (IL-1 receptor family and alarmins) and the upregulation in the same patients of genes of the adaptive immunity related to B and T lymphocytes activation. A transcriptional regulation was observed also for genes with antimicrobial function and protease activity and for genes involved in carbohydrate metabolism, lipid inflammatory pathway, transport of vesicles and protein synthesis. miR-125a-5p and miR-150-5p, with a predicted regulatory role in the MAPK pathway, and miR-193a-3p were differentially expressed in the acute and steady state condition.

Conclusion

We observed a significant modulation of multiple classes of genes involved in defense response to pathogens, immunity, inflammation and metabolism. From these results it appears that in septic shock a relevant change in the transcriptomic profile of blood cells is induced, in order to counteract the pathogens and as a consequence of the hemodynamic changes underlying the circulatory failure. The transcriptomic profile of septic shock patients showed inter patient variability reflecting the complexity of the shock condition and of the individual response to treatment. Specific signatures

could turn out by combining clinical data and expression profile and could be used to better classify septic shock patients.

INDEX

1 INTRODUCTION

1.1 Sepsis and septic shock

Sepsis is defined as a life-threatening organ dysfunction caused by a dysregulated host response to infection [1]. Sepsis accounts for one million cases annually in the United States and it is the most frequent cause of mortality in intensive care units (ICUs) [2]. Sepsis most often occurs in patients with underlying disabilities or illnesses and can originate from either bacterial or fungal or viral infection. The most common cause of sepsis are bacterial infections due to Gram-positive (52.1 %) or Gram-negative bacteria (37.6%), whereas fungal infections are less frequent (4.6%) but they are increasing compared to the past [3]. Sepsis can arise from multiple kind of infection: Esper et al. reported that in the 25 year period from 1979 to 2003 the most frequent types of infection in sepsis and septic shock were respiratory (33%), genitourinary (32%) or gastrointestinal (23%) infections [4]. The identification of the causative organism can be missing in some patients and this is due to the fact that, by the time they are admitted to the ICU, they have already been treated with antibiotics[5].

Septic shock is a complication of sepsis in which underlying circulatory and cellular/metabolic abnormalities are profound enough to substantially increase mortality at 40% or more. The shock condition is characterized by pronounced hypotension, with systolic blood pressure <90mmHg or mean arterial pressure <65mmHg. Besides the specific antimicrobial therapy, patients are treated with vasopressors to maintain Mean Arterial Pressure > 65mmHg. [1]. Hyperlactatemia is a common finding in septic shock patients and plasma lactate levels and their trend overtime are reliable markers of severity and mortality[6]. The majority of patients with shock develop multiple organ dysfunction syndrome (MODS), a condition in which organs not

directly affected by the original infection become dysfunctional. This ultimately represents the main cause of death[7].

The course of sepsis is variable and often unpredictable and depends on factors such as age and pre-existing morbidities. Incidence rates for sepsis are known to increase with age[8], probably due to age-related differences in immune function, ranging from failed antigen processing by leukocytes[9] to altered inflammatory cytokine expression[10]. In sepsis, mortality depends on age and on the duration of the ICU stay: patients >55 years of age and those who remained in the ICU for >14 days have the highest post-discharge mortality rates. Mortality rates in septic shock also depends on expertise and experience of the treating center and range from 20 to 50 % depending on the country [11]. Only a minority of survived patients return to a normal life: survivors are frequently affected by cognitive dysfunction, neuropathies, myopathies, immunological dysfunction and other complications and they are at risk for early death within 5 years, with mortality rates as high as 75%[12]. Possible reasons of these functional and physical declines might include ICU-acquired weakness owing to both inactivity and immobilization, as well as from inflammation, corticosteroid and neuromuscular blockers commonly used in sepsis treatment[13].

1.2 Patient treatment in Intensive Care Unit

In the treatment of sepsis the antimicrobial therapy is of primary importance: an initial appropriate antimicrobial therapy significantly reduces mortality risk and a broad spectrum of antimicrobial treatments covering all likely organisms should be started as soon as possible [14]. For what concerns the treatment of hypotension in septic shock, current therapies are targeted to restore an adequate level of perfusion in order to prevent organ failure: septic shock patients require the administration of fluids (crystalloids) and vasoactive agents (e.g. noradrenaline) in order to avoid prolonged

hypotension and they receive lung support with a ventilator in order to achieve adequate oxygenation. A crucial point is the protection of the heart and preservation of its function which is important to ensure hemodynamic stability and an adequate perfusion to all vital organs. In the ICU the severity of organ dysfunction can be assessed with a scoring system that quantifies disease severity according to clinical findings, laboratory data or therapeutic interventions. The predominant score in current use is the Sequential Organ Failure Assessment (SOFA)[15]. The score provides an assessment of the dysfunctions regarding liver, kidney, cardiovascular and central nervous system, respiration and coagulation and accounts for clinical interventions and laboratory variables like PaO2, platelet count, creatinine level, and bilirubin level. A higher SOFA score is associated with an increased mortality.

1.3 Pathophysiology of sepsis

In infection, the invading microbial pathogens are recognized by the host through pattern recognition receptors (PRRs). PRRs are expressed on innate immune cells such as polymorphonuclear neutrophils (PMNs), monocytes/macrophages and on epithelial and endothelial cells as well. PRRs recognize the presence of highly conserved and unique structures of microbial pathogens called pathogen-associated molecular patterns (PAMPs) as well as detect endogenous damage-associated molecular patterns (DAMPs) generated in the setting of cellular damage or tissue injury[16], [17].

Examples of PAMPs are lipopolysaccharide (LPS) or lipid A, lipoteichoic acid (LTA), carbohydrate moieties, double-stranded RNA and unmethylated DNA motifs. At least five major classes of PRRs are known, which include two families of membrane-bound PRRs: Toll-like receptors (TLRs) and C-type lectin receptors (CLR), and three families of cytoplasmic PRRs: the nucleotide binding and oligomerization domain (NOD)-like receptors (NLRs),

retinoic acid-inducible gene (RIG)-I-like receptors (RLRs) and absence in melanoma 2 (Aim 2)-like receptors [18], [19]. Upon PAMP engagement, PRRs trigger a complex intracellular signaling system involving phosphorylation of mitogen-activated protein kinases (MAPKs), Janus kinases (JAKs), signal transducers and activators of transcription (STATs) and nuclear translocation of nuclear factor-κB (NF-κB). Early response genes are expressed, including cytokines associated with inflammation (TNF, IL-1, IL-12, IL-18 and type I interferons (IFNs)) and the complement system is activated[13]. Monocytes/macrophages, PMNs and dendritic cells (DCs) can target pathogenic microorganisms through phagocytosis or by releasing substances such as inflammatory cytokines, chemokines, adhesion molecules, reactive oxygen species (ROS) and other mediators. The elimination of microbial pathogens from the host can result in an overwhelming inflammatory response, with the loss of normal immune homeostasis, which ultimately causes tissue damage and organ dysfunction[20]. As a form of protection, a period of immune hypo-responsiveness, also known as endotoxin tolerance, can occur with repeated LPS stimulation and is associated with the reduced survival seen in patients with septic shock[21].

Danger-associated molecular patterns (DAMPs, or alarmins) derived from host products within cells are sensed by retinoic acid inducible gene 1–like receptors (RLRs) and nucleotide-binding oligomerization domain-like receptors (NLRs), with promotion of the assembly of inflammasomes. DAMPs implicated in sepsis pathogenesis include high-mobility group protein B1 (HMGB1), S100 proteins, extracellular RNA, DNA, and histones. Inflammasome mediates the release of HMGB1, IL- 1b, and IL-18, which are secreted into the extracellular space and function to amplify the innate immune response ([22] and mediate pyroptosis, a form of programmed cell death.

The inflammatory response is a highly evolutionarily conserved system that is activated following a harmful stimulus like infection or injury and needs to be closely regulated. If the response exceeds a certain threshold, a systemic injury can occur. Reactive oxygen species (ROS) can damage cellular proteins, lipids and DNA and impair mitochondrial function, whereas the complement activation can further increase the generation of ROS, granulocyte enzyme release, endothelial permeability and tissue factor expression and may cause the death of adrenal medullary cells[23]. A profound effect is observed on coagulation and on the vascular and lymphatic endothelium where there is increased expression of selectins and adhesion molecules. The integrity of the endothelium is diminished due to neutrophils and platelets enhanced adhesion, to the release of inflammatory mediators and toxic oxidative and nitrosative intermediates. The response produced by sepsis enables platelets and leukocytes to reach tissue sites in response to trauma or localized infection, but the produced effect is so prolonged, excessive and generalized that it can lead to a considerable tissue injury. The endothelial dysfunction and the alterations of the glycocalix (a layer that covers the endothelium and supports the anticoagulant state and maintain tight junctions) promote coagulation characterized by microvascular thrombi, fibrin deposition, neutrophil extracellular trap formation. In sepsis and septic shock the leaky capillary membranes create massive loss of intravascular proteins and plasma fluids into the extravascular space. The vasodilation of the small blood vessels impairs the microcirculation resulting in a poor tissue perfusion. The widespread immunothrombosis can result in disseminated intravascular coagulation (DIC) with impairment of the microvasculature function and organ injury[24]. The interrelationship between inadequate oxygen delivery to peripheral tissues, ischemia and reperfusion injury in the organs, hemodynamic instability, inflammation and development of MODS has been extensively

investigated, but the molecular mechanisms which ultimately trigger tissue functional injury remain largely undetermined[25].

Sepsis can affect all organs of the body: patients often present decreased lung compliance with increased respiratory rate due to inflammatory-induced damage to alveolar capillary membranes with generation of pulmonary oedema. Myocardial depression is induced by mechanisms involving cytokines and nitric oxide or through cardiomyocytes injury induced by toxins, complement and DAMPs [Figure 1] [26].

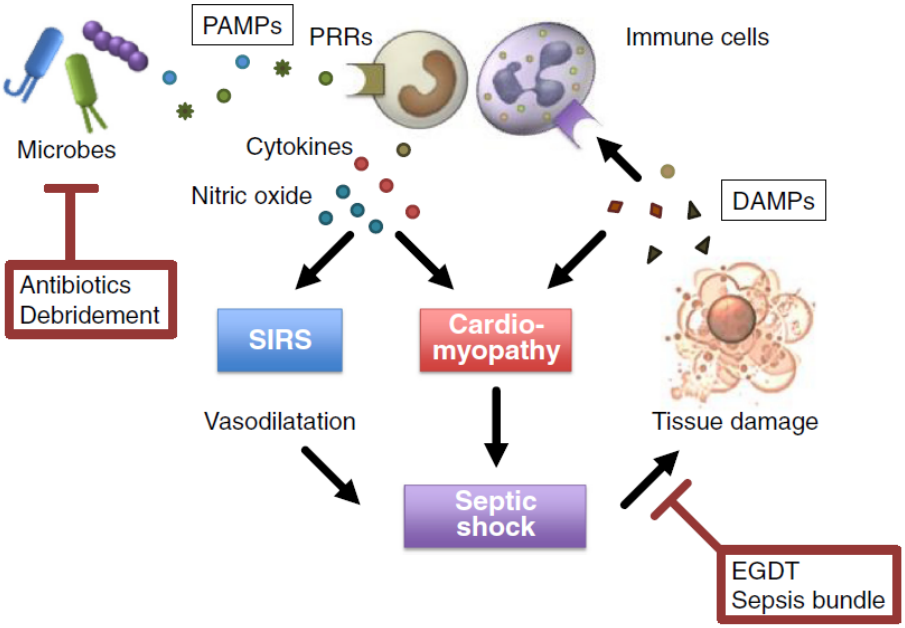

Figure 1 Management of myocardial dysfunction in septic shock. Prompt and adequate antibiotic therapy is important to decrease PAMPs arising from invasive microorganisms. Antibiotics Early goal-directed therapy (EGDT), including fluid resuscitation, vasopressor and inotropic therapy, and red blood cell transfusion, is important to re-establish organ perfusion pressure, which helps to maintain blood flow to tissues and reduces the release of damage-associated molecular patterns (DAMPs) in patients with septic shock [26].

The high levels of cytokines make the gut epithelium more permeable and the luminal content containing activated pancreatic proteases enzyme induces injury in the gut (autodigestion) and cause various degrees of cell and organ dysfunction that can reach the point of complete organ failure [27]. In the liver, sepsis impairs hepatocyte clearance of bilirubin and other crucial hepatic functions including the transport and processing of enteric pathogen lipids, further stimulating systemic inflammation[28]. In kidneys, cytokines and immune system mediate microvascular and tubular dysfunction resulting in acute kidney injury (AKI) [29] which is common in severe sepsis and increases the risk of death[30]. Severe sepsis patients typically present altered mental status with brain dysfunctions ranging from mildly impaired concentration to deep coma [31]. Systemic endothelial dysfunction compromises the blood-brain barrier, allowing inflammatory cytokines and cells to enter the brain, causing perivascular edema, oxidative stress, and neurotransmitter alterations. Areas of ischemia and hemorrhage can appear in the brain due to coagulopathy and impaired regulation of cerebral blood flow[32]. In addition the CNS is reached by a toxin influx due to hepatic and renal dysfunction.

In sepsis the early proinflammatory state often develops into a later and prolonged state of immune system dysfunction. In septic patients, lymphocytes decrease their number and persisting lymphopenia after the onset of sepsis is a predictor of mortality[33]. Neutrophils acquire an immature phenotype with impaired phagocytosis[34] and myeloid-derived suppressor cell (MDSC) population is expanded[35]. Both immature blood neutrophils and MDSCs secrete anti-inflammatory cytokines, including IL-10 and transforming growth factor-β (TGFβ), which further suppress immune function [Figure 2] [13]. Monocytes decrease the capacity to release proinflammatory cytokines such as TNF, IL-1α, IL-6 and IL-12, in response to LPS (endotoxin tolerance)[21]. LPS can still activate monocytes but they

are shifted towards the production of anti-inflammatory molecules such as IL-1 receptor antagonist (IL1-RA) and IL-10. Circulating antigen-presenting cells (APCs) lose the expression of the human leukocyte antigen-antigen D related (HLA-DR)[36] resulting in reduced antigen presentation and they increase the surface expression of inhibitory T cell ligands suppressing T cell function[35]. In response T cells skew their activation state to a immunosuppressive T helper 2 phenotype causing T cell anergy.

In a post mortem study of sepsis patients, apoptotic cell death was identified as a main factor underlying immunosuppression with loss of T cells, B cells and dendritic cells. Accordingly, a decrease of sepsis induced apoptosis, through pharmacological or genetic interventions, improve survival in animal models of sepsis[37]. Apoptosis of immune cells occurs in lymphoid tissues (spleen, thymus and lymph nodes) and gut-associated lymphoid tissues (GALTs)[38]. The damaging effects of apoptosis are not only due to the loss of immune cells but also to the impact that apoptotic cells have on the surviving immune cells. Uptake of apoptotic cells by monocytes, macrophages and dendritic cells induces immune tolerance, anergy or a T helper 2 (TH2) cell-associated immune phenotype[39], [40].

Recent post-mortem studies have reported that a high number of patients who die of sepsis have unresolved opportunistic infections[41] due to a marked immunosuppression and during the course of the illness multiple viruses are often reactivated (cytomegalovirus, Epstein-Barr virus, herpes simplex virus)[42].

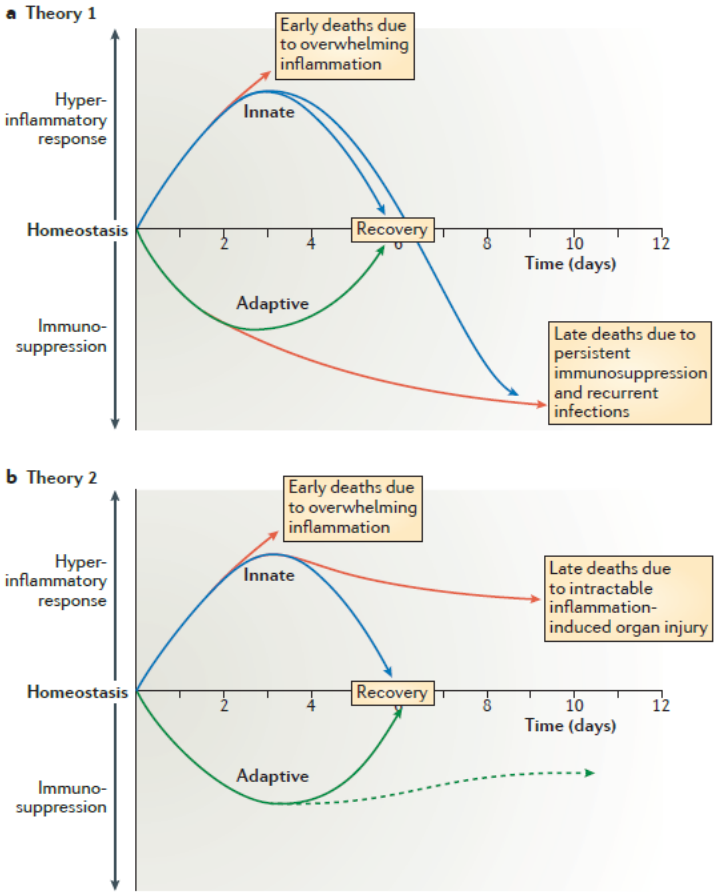

Figure 2 A) Theory 1: Cells of the innate immune system, including monocytes and neutrophils, release high levels of pro-inflammatory cytokines that drive inflammation (blue line; days 1–3). The intensity of the initial inflammatory response varies in individual patients depending on multiple factors, including pathogen load and virulence, patient co -morbidities and host genetic factors. Early deaths in sepsis (top red line; day 3) are typically due to a hyperinflammatory 'cytokine storm' response with fever, refractory shock, acidosis and hypercatabolism. Most patients have a restoration of innate and adaptive immunity and survive the infection (recovery; blue and green lines; day 6). If sepsis persists, the failure of crucial elements of both the innate and the adaptive immune systems occurs such that patients enter a marked immunosuppressive state (blue and red lines; after day 6). Deaths are due to an inability of the patient to clear primary infections and the development of secondary infections. B) Theory 2: a competing theory of sepsis agrees that there is an early activation of innate immunity and a suppression of adaptive immunity; however, this theory holds that deaths in sepsis are due to the persistent activation of innate immunity that results in intractable inflammation and organ injury. According to this theory, late deaths in sepsis are due to persistent, underlying innate immune-driven inflammation[43].

1.4 Metabolic dysfunction

Patients with sepsis have damaged and dysfunctional mitochondria damaged by high levels of ROS[44]. At the cellular level a generalized reduction of energy expenditure is observed, which probably increases organ dysfunction as many viable cells reduce their efficiency in performing their specialized functions. This is involved in development of acute kidney injury, myocardial depression, hepatic dysfunction, encephalopathy, acute lung injury and decreased barrier and transport functions of the gastrointestinal tract [45]. Catabolism is another characteristic of severe sepsis. A prospective study of 63 critically ill patients in England documented rapid and substantial loss of muscle mass, especially in patients with multiorgan failure [46]. The breakdown of muscle tissue releases amino acids converted into glucose through the gluconeogenesis pathway which fuels the glucose dependent proliferation of innate immune cells. The insulin insensitivity and hyperglycemia characteristic of sepsis and critical illness may have evolved to ensure that glucose levels are adequate to support the massive immune response [47]. Serum lactate level is increased, which is considered a marker of cellular metabolic abnormality and a criteria to define septic shock. Other metabolic alterations reported in different settings of septic shock patients regard circulating kynurenine, fatty acids, lysophosphatidylcholines species and/or carnitine esters [48]–[50], pointing toward an overall derangement of energy circuits and lipid homeostasis.

1.5 Sepsis Biomarkers

Biomarkers are molecular indicators that can be used for diagnosis or to predict the outcome. In biological homeostasis their measurement is in a reference window, consequently they are useful for identifying abnormal processes and are important factors in the decision-making process of disease assessment. Commonly used biomarkers for sepsis include C-reactive protein (CRP) and procalcitonin (PCT), cytokines (tumor necrosis factor (TNF)-α, interleukin (IL)-1, IL-6, IL-10, osteopontin), chemokines (macrophage migration inhibitory factor (MIF), high-mobility-group box 1), and soluble receptors (soluble triggering receptor expressed on myeloid cells 1 (sTREM-1), soluble urokinase-type plasminogen activator receptor (suPAR)) [51]. In clinical practice the use of a single biomarker doesn't satisfy all requirements for sepsis diagnosis and treatment management because sepsis has a complex pathophysiology that involves hundreds of mediators. The use of emerging omics tools is particularly promising for complex and heterogeneous conditions such as septic shock. The systematic identification of sepsis biomarkers and examination of the molecular mechanisms underlying sepsis using omics approaches may provide insights into the physiological state of patients following infection. The use of multiple omics (i.e. transcriptomics, proteomics, metabolomics) could provide integrated information on particularly significant biomarkers, help to better understand the complex pathogenesis of the disease, its evolution and to develop tools for the effective diagnosis and to improve prognosis.

2 AIM OF THE WORK

The aim of the present work, that has been performed in the frame of the European Project ShockOmics (HEALTH.2013.2.4.2-1), is to analyze the transcriptome of a cohort of 32 septic shock patients recruited in two Intensive Care Units (ICUs) in Europe at multiple timepoints of the clinical course.

In detail we aimed to:

- evaluate the blood gene expression at the time of ICU admission, at day 3 and day 7 of the ICU stay with RNA sequencing

- apply the Principal Component Analysis and Unsupervised Hierarchical Clustering to explore the transcriptomic dataset

- analyze the differential expression of protein coding transcripts, long non coding RNAs and microRNAs

- identify biological processes and pathways modified during the clinical course of septic shock

3 MATERIALS AND METHODS

3.1 Patient recruitment and inclusion criteria

Septic shock (SS) patients were recruited in the Intensive Care Units (ICU) of two Clinical Centers, Hôpitaux Universitaires de Genève (Switzerland) and Hôpital Erasme, Université Libre de Bruxelles (Belgium).

3.1.1 Inclusion criteria

SS Patients included in the study were selected using the following criteria:

- Septic Shock Severity: patients with SOFA > 5
- First blood sample and first hemodynamic measurements available within 16 hours from admission to the ICU.
- Informed Consent available: the consent is requested to the patient, or to its relatives in case of altered consciousness, and signed by the physicians in the ICU. Delayed consent may be asked according to local rules and regulations in case the relatives were unavailable at the time of potential enrollment.

3.1.2 Exclusion criteria

Patients were excluded from the study according to the following criteria:

- Risk of fatal illness and death within 24 hours
- Patients already enrolled in other studies
- Active hematological malignancy or active cancer
- Immunodepression: including transplant patients, patients positive to HIV virus; constitutive immune system deficiency, subministration of immunosuppressive therapy, including systemic corticosteroids (aerosols allowed).
- Patients receiving plasma or whole blood

- Patients with pre-existing end stage renal disease needing renal replacement therapy (RRT), or chronically treated by intermittent dialysis.
- Cardiac surgery in the previous ten days
- Cirrhosis (Child-Pugh C) or acute liver failure

3.1.3 Samples collection Timing guidelines

The diagnosis of shock occurred either when patients are admitted to the ICU or after admission if they were previously admitted to the ICU without shock symptoms.

Timing for the collection of blood samples for transcriptomics analysis [Figure 3]:

- Time 1 (Acute Shock): time at which the first blood sample for analysis is collected, within 16 h after ICU admission. This time point is considered representative of acute shock before the therapy has taken effect, when shock has already activated the main patho-physiological cascades of inflammation and disease;
- Time 2 (Post Treatment): time at which first blood sample is collected, at 48 h after ICU admission. At this time point, the treatment has been administered for a sufficient time to evaluate its effects on the early molecular markers of disease;
- Time 3 (Steady State): time at which the third blood sample for analysis is collected, on day 7 of the ICU stay of the patient or before discharge from the ICU in case of shorter stays or before discontinuing therapy (death). At this time point, it is assumed that the molecular pathways previously affected by the pathological condition have reached a steady state.

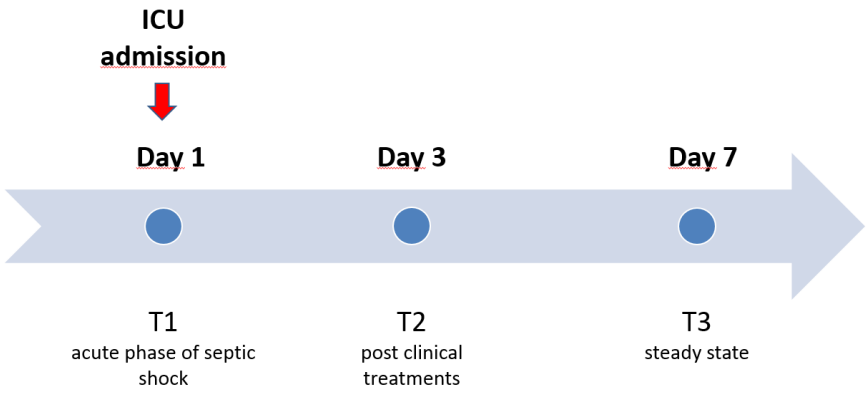

Figure 3 Experimental scheme showing the timing of blood samples collection for transcriptomics analysis.

3.1.4 Clinical data

All the clinical data of each patient participating in the study are documented in the Case Report Form (CRF). Medical records were maintained anonymous using an alphanumeric hash code. All data collected in the CRFs were stored in a database and made available in tabular format. The clinical database shows patients at specific timepoints (rows) and clinical variables (columns).

Clinical variables include records of:

- demographics and comorbidities
- blood pressure and heart rate
- severity scores (SOFA, APACHE II at Time 1, 2, 3)
- evaluation of Acute Heart Failure (AHF) assessed by a series of measures of cardiac function, cardiac output monitoring, lactate level and/or inotropic drugs weaning, velocity time integral (VTI) using echocardiography.
- previous therapy

- temperature
- on going therapy (drugs, fluids, etc…)
- cardiorespiratory assistance (mechanical ventilation, extracorporeal membrane oxygenation, intra-aortic balloon pump, etc.)
- biochemical parameters (creatinine, bilirubin, lactate, glycemia, complete blood count, coagulation markers, arterial blood gas analysis)
- assessment of organ failure
- cognitive assessment by Glasgow Coma Scale
- survival in hospital, at 28 days and 100 days

3.2 Laboratory protocols

3.2.1 Blood collection and RNA extraction

At timepoints T1, T2, T3, 1 ml of venous blood was collected from each patient in EDTA tubes and kept on ice. Immediately after, 400µl of whole blood were added to 400 µl of Denaturing solution (Ambion, USA), in duplicate. Total RNA was extracted from 800 µl of treated blood with MirVana Paris Kit (Ambion, USA). RNA was treated with TURBO DNA-free Kit (Ambion, USA) in order to remove any DNA contamination. RNA Quality Control was performed on all RNA samples with an electrophoretic run on Agilent Bioanalyzer instrument using the RNA 6000 Nano Kit (Agilent, Santa Clara, CA)[Figure 4]. RNA Integrity Number has been determined for every sample and all the samples were considered suitable for processing based on the RNA integrity (RIN > 7). RNA concentration was estimated through spectrophotometric measurement using a Nanoquant Infinite M200 instrument (Tecan, Austria).

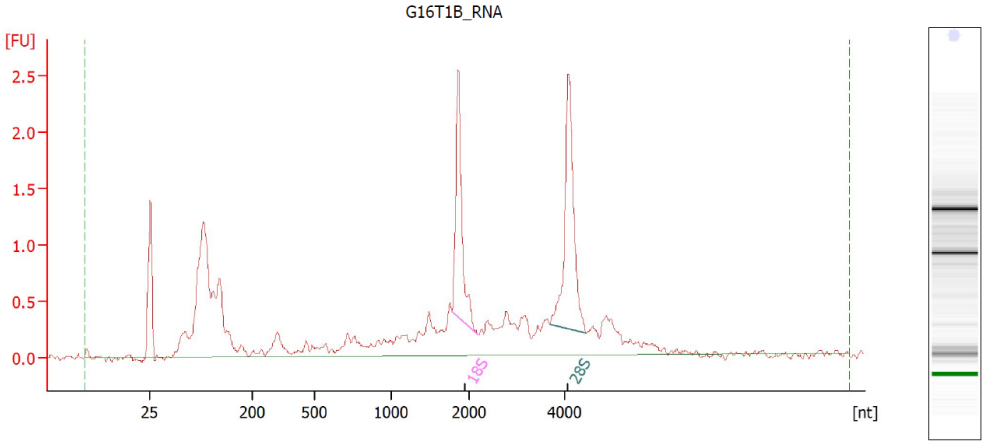

Figure 4 RNA quality control. Electrophoretic run on RNA6000Nano chip with Agilent Bioanalyzer. The RNA sample shows two peaks at 2000 nt and 4000 nt corresponding to ribosomal RNAs 18S and 28S. A strong signal corresponding to the smallRNA fraction is visible in the region between 25 nt (molecular marker) and 200 nt. On the right the gel-like picture.

3.2.2 Library preparation for RNA sequencing

Whole transcriptome sequencing libraries were prepared using the TruSeq Stranded Total RNA with Ribo-Zero Globin Kit (Illumina, San Diego, CA) using 800 ng of total RNA as input. The kit uses oligo-attached magnetic beads to remove rRNA and globin mRNA from total RNA. The remaining RNAs were purified, fragmented at 94°C for 8 minutes and primed with random hexamers for cDNA synthesis. Multiple indexing adapters were ligated to the ends of ds cDNAs that were then amplified with 11 PCR cycles. Final libraries were validated and quantified with the DNA1000 kit on Agilent Bioanalyzer Instrument [Figure 5]. Pooled libraries were sequenced on the HiSeq2500 Instrument producing 50x2 bp paired end reads.

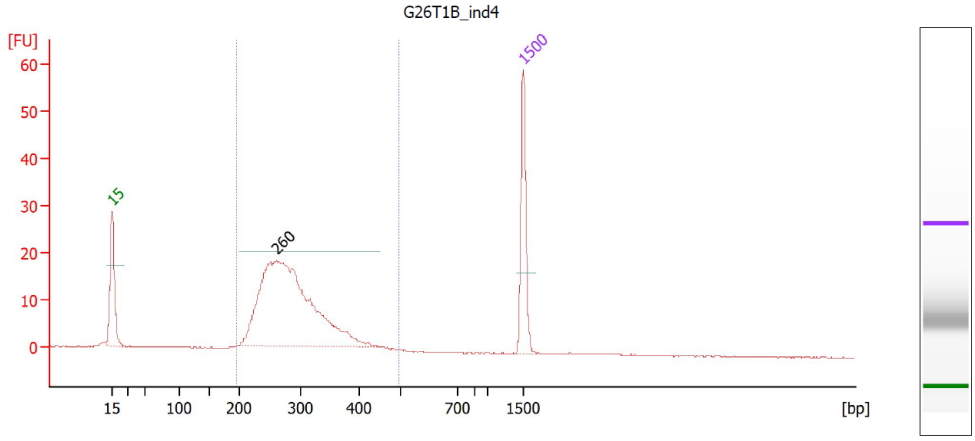

Figure 5 Library quality control. Electrophoretic run of a RNASeq library on DNA1000 chip with Agilent Bioanalyzer showing a typical distribution skewed to the right. Molecular markers at 15 nt and 1500 nt. On the right the gel-like picture.

3.2.3 Library preparation for SmallRNA sequencing

Small RNA sequencing libraries were prepared using the TruSeq SmallRNA Library Prep Kit (Illumina, San Diego, CA) using 500 ng of total RNA as input. Adapters were sequentially ligated to 3' and 5' of the RNA molecule and an RT reaction was used to create single stranded cDNA. The cDNA was then amplified with 8 PCR cycles using a common primer and a primer containing 1 of 48 index sequences. After purification using Agencourt XP beads, libraries were validated and quantified with the High Sensitivity DNA kit on Agilent Bioanalyzer Instrument [Figure 6]. Indexed libraries were mixed according to their concentration in order to create an equimolar pool. The library pool was run in a polyacrylamide gel (Novex TBE gel 6%, Life Technologies) and the microRNA fraction was isolated with a gel cutter. The final pooled library was validated with the High Sensitivity DNA kit on Agilent Bioanalyzer Instrument [Figure 7] and sequenced on the NextSeq Instrument producing 50bp single end reads.

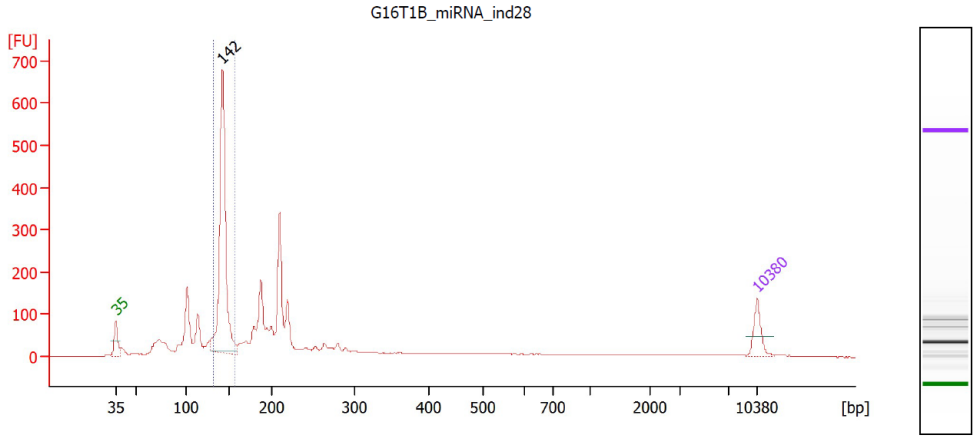

Figure 6 Library quality control. Electrophoretic run of a SmallRNA library on High Sensitivity DNA chip. The library shows multiple peaks in the region up to 300 nt. The region of the highest peak (142 nt) corresponds to the typical size of a library fragment containing a miRNA insert. The insert length can be calculated subtracting the length of the adapter molecules (120 nt) from the fragment length estimated with the electrophoretic run. Molecular markers at 15 nt and 10380 nt. On the right the gel-like picture.

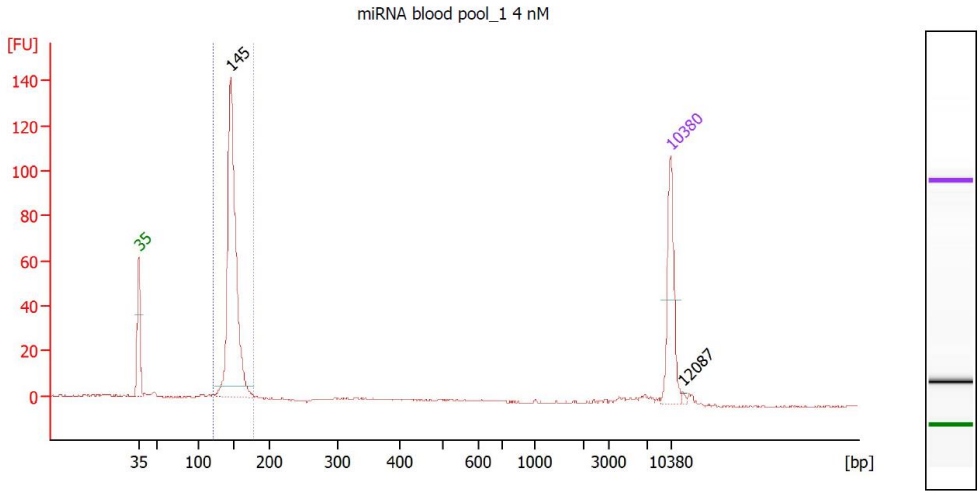

Figure 7 Library quality control. Electropherogram of a smallRNA library after size selection and enrichment for microRNA fragments. The estimated size of the library is around 145 nt corresponding to a insert size coherent with the expected length of miRNA molecules (20-26 nt). Molecular markers at 15 nt and 10380 nt. On the right the gel-like picture.

3.3 Sequencing data analysis

In order to catch most of the shock transcriptomic features at molecular level, we performed RNA sequencing of whole transcriptome including mRNAs, long ncRNAs and small-RNAs (microRNAs).

3.3.1 Transcriptomic data analysis workflow

Whole blood RNA libraries were sequenced in six batches on HiSeq Illumina Platform. The bioinformatics workflow includes three core modules [Figure 8]:

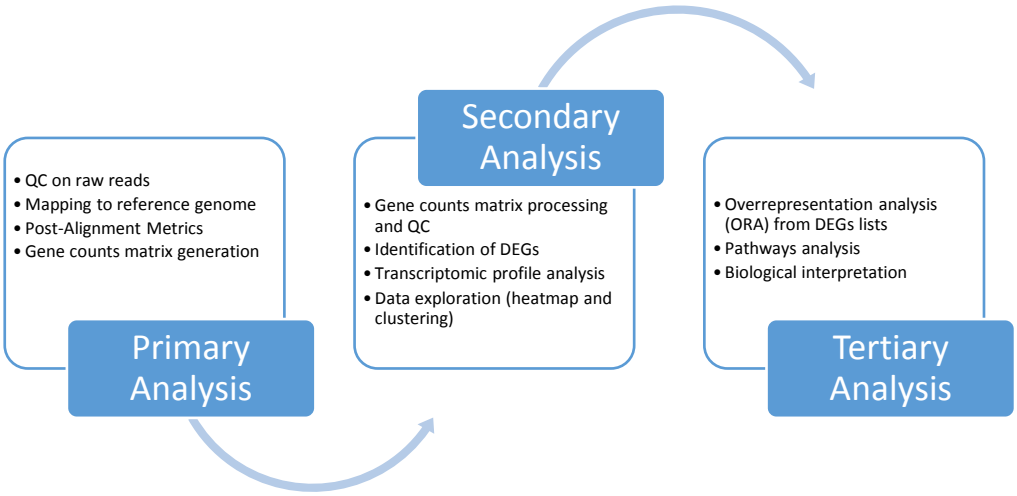

Figure 8 Analysis workflow for transcriptomic data

1. A primary analysis which creates the counts matrix
2. A secondary analysis that explores the transcriptomic dataset and identifies differentially expressed genes (DEGs) according to the experimental design

3. A ternary analysis that consists in bioinformatic downstream analyses, that starts from the identified list of DEGs and ends with the biological interpretation of the results.

In the next paragraphs, methods and procedures of each part are described.

3.3.1.1 Primary analysis

The starting point of the analysis is the quality check of raw reads produced by the sequencing platform. Raw reads are stored in the FASTQ format. In this format, each read is described by four consecutive lines: sequence identifier, raw sequence (ATCG), + character line and corresponding quality score (ASCII encoding) of sequence read at 2nd line. Every sequenced sample comes with two FASTQ files corresponding to the two different strands (forward and reverse).

We performed the quality control procedure using FASTQC (v11.2) in order to check several metrics, specifically focusing on the evaluation of base quality score distribution across reads length.

3.3.1.1.1 RNASeq data

Quality checked reads were mapped using STAR aligner (v2.5.2) using the GENCODE primary assembly genome as reference genome and the GENCODE evidence-based annotation of the human genome (GRCh38), version 24 (Ensembl 83). Mapping was setup in order to output only reads mapping uniquely to a single genomic coordinate. All reads mapping to multiple loci were discarded from downstream analysis. Once mapped, several post alignment metrics were performed in order to check coverage distribution across gene length, ribosomal RNA (rRNA) depletion efficiency, DNA contamination and number of genes detected. All these metrics were collected using RNAseq-QC software[52]. Samples failing post alignment quality control metrics were resequenced. The primary analysis ends with

genes counts matrix creation. This step is fundamental to quantitatively determine how many fragments (reads pair) cover each single gene. Counting is not a trivial operation because mapped reads can be splitted over two or more exons or can overlap more than one gene. This process was performed using featurecounts module implemented in the subread software[53]. Parameters were setup accordingly, in order to count only fragments that map unambiguously to a single gene and taking into account strand information.

3.3.1.1.2 SmallRNA sequencing data

FASTQ files were converted into FASTA files and adapter sequences were removed using perl scripts. Sequences of 2588 human mature microRNAs were downloaded from miRBase 21 database. Only reads perfectly matching miRBase microRNA sequences were considered and used to produce count expression values.

3.3.1.2 Secondary analysis

The second step of the bioinformatics analysis was centered on the study of the transcriptomic profiles and on the identification of differentially expressed genes (DEGs) by comparing different conditions according to the experimental design. Gene counts matrix was mainly processed and analyzed by using DESeq2 R package[54].

3.3.1.2.1 DESeq2 theory

DESeq2 suite offers a general solution for gene-level analysis of RNA-Seq data. DESeq2 performs well both in experiments with a small number of samples and with many samples. The DESeq2 models read counts K_{ij} as following a Negative Binomial distribution with mean μ_{ij} and dispersion α_i. Terms are modelled through a generalized linear model (GLM) of the form:

$$K_{ij} \sim NB\ (mean = \mu_{ij}\ , \text{dispersion} = \ \alpha_{ij}\ )$$

In the count matrix K each row i represent a gene, whereas at column j there are the samples. Hence, K_{ij} indicates the number of unique unambiguously mapped reads that map to the gene i in sample j. The NB distribution has mean μ_{ij}, which is the quantity q_{ij} that is proportional to the cDNA concentration in the library scaled by a normalization factor s_{ij} which takes into account the total amount of cDNA sequenced in the sample j. In formula the mean of the NB for the gene i and sample j is:

$$\mu_{ij} = s_{ij} * q_{ij}$$

The purpose of the size factors s_j is to render counts from different samples, which may have been sequenced to different depths, comparable. Hence, the ratios $EK_{ij}/EK_{ij'}$ of expected counts for the same gene i in different samples j and j′ should be equal to the size ratio $s_j/s_{j'}$ if gene i is not differentially expressed or samples j and j′ are replicates. The total number of reads, $\sum_i K_{ij}$ could be a good measure of sequencing depth and hence a reasonable choice for s_j. Experience with real data, however, shows this not always to be the case, because a few highly and differentially expressed genes may have strong influence on the total read count, causing the ratio of total read counts not to be a good estimate for the ratio of expected counts. Size factors are then estimated using the median-of-ratios method. This method relies on the creation of a reference pseudosample in which gene by gene the value of expression for the each gene is the geometric mean of the counts of all samples in that gene. Hence, the size factors vector results as the median (across all genes) of the ratios between observed counts and the value of the pseudocount of each sample. One size factor for sample. In formula:

$$\hat{s}_j = \underset{i}{median} * \frac{k_{iv}}{(\prod_{v=1}^{m} k_{iv})^{\frac{1}{m}}}$$

The coefficients β_i give the log_2 fold changes for gene i for each column of the model matrix X.

$$log_2(q_{ij}) = x_j \beta_i$$

The second parameter needed in the algorithm is the coefficient of dispersion α_i. This coefficient describes the relationship between the variance of the observed count and its mean value:

$$Var\, K_{ij} = \mu_{ij} + \alpha_i \mu_{ij}^2$$

The log_2 fold changes in β_i are the maximum a posteriori estimates after incorporating a zero-centered Normal prior providing a moderated log_2 fold change estimates. Dispersions are estimated using expected mean values from the maximum likelihood estimate of log_2 fold changes, and optimizing the Cox-Reid adjusted profile likelihood.
The steps performed by the DESeq2 are the following:

1. estimation of size factors s_j by estimateSizeFactors
2. estimation of dispersion α_i by estimateDispersions
3. negative binomial GLM fitting for β_i and Wald statistics by nbinomWaldTest or Likelihood Ratio Test

3.3.1.2.2 Data transformation

In order to analyze and explore expression data by clustering and principal components analysis techniques is necessary to transform data. Typically,

in RNA-Seq data are heteroskedastic that is the variance grows with the mean. Common statistical methods for exploratory analysis of multidimensional data, especially methods for clustering and ordination (e.g., principal-component analysis), work best for (at least approximately) homoscedastic data; this means that the variance of an observable quantity (i.e., here, the expression strength of a gene) does not depend on the mean. For example, if PCA is performed directly on a matrix of normalized read counts, the result typically depends only on the few most strongly expressed genes because they show the largest absolute differences between samples. A simple and often used strategy to avoid this is to take the logarithm of the normalized count values plus a small pseudocount ($\log_2$(normcounts) + 1). In this situation, however, genes with low counts tend to dominate the results because, due to the strong Poisson noise inherent to small count values, they show the strongest relative differences between samples. To avoid that a few highly variable genes dominate the distance measure, and have a roughly equal contribution from all genes, we used the regularized log-transformation (rlog) that stabilize the variance of the data and make its distribution roughly symmetric and suitable for exploratory analysis. The rlog transformation at high counts is pretty equal to an ordinary log2 transformation but at low counts stabilizes the variance.

3.3.1.2.3 PCA Analysis

Principal Component Analysis was performed using the plotPCA function in deseq2 package. The function is a wrapper function that call prcomp function on deseq2 transformed data. PCA was performed using top 5000 most variable genes from the regularized log transformed object. 2D PCA plots were generated showing the percentage of variability explained by the 1st and the 2nd components. Patients were colored by the time point variable.

3.3.1.2.4 Heatmap generation

In order to view and explore the transcriptional signature that allow to discriminate group of patients, we used heatmap plot. Heatmap plot is a graphical representation of data where the individual values contained in a matrix are represented as colors. Rows represent genes, whereas columns represent samples. The color of the tile T_{ij} represents the z-score of the expression values distribution for sample i at gene j. Every gene has its own distribution. The data from which the heatmap is drawn is the matrix of $\log_2$ normalized counts plus 1 in order to avoid missing values for log2 values less than 1. Normalized counts matrix is calculated using median of ratios method as previously explained.

$$log_2(normalized\ counts + 1)$$

In particular, pheatmap function was used to create all the heatmaps. Using rlog counts instead of log2(normalized counts + 1) is not necessary in this approach because low counts values tend to be absent in differentially expressed genes list. All heatmaps were drawn organizing tiles using hierarchical clustering at sample / patient level. In this way is possible to easily identify which group of genes allow to discriminate transcriptomics profiles at sample level. By using also hierarchical clustering to organize tiles on the heatmap the user can instead identify more clearly which are the group of genes that share the same expression signature across samples investigated. Note that hierarchical clustering at sample level (columns) is not affected by enabling hierarchical clustering at gene level (rows). Briefly the hierarchical clustering was setup using Euclidean distance as method to create distances matrix and complete method as the aggregation method for clustering.

3.3.1.2.5 Differential expression analysis

Differential expression analysis was performed using a two-stage procedure. The first stage aimed to identify genes whose expression changes across timepoints, in order to identify the genes that can potentially characterize the severity of a specific timepoint. The second stage focuses on identifying differentially expressed genes between extreme conditions, acute phase (T1) and recovery phase (T3). First-stage DEGs analysis aims to answer the following question: which are the genes that significantly change their expression across time, considering that for each sample all three timepoints are available? To answer this question, we performed the DEGs analysis using the nbinomLRT function implemented in deseq2 package. This function tests for significance of change in deviance between a full and reduced model.

Full model is represented by the following design formula:

$$\sim patient + timepoint$$

With this formula, we model counts taking care of patient and timepoint. Reduced model is instead described by this one:

$$\sim patient$$

As we can see in the reduced model, the timepoint variable is not present anymore. In this way we model counts taking care only on the sample variable, that is equal to say that time does not contribute to model counts.

The difference in deviance is compared to a chi-squared distribution with degrees of freedom = (reduced residual degrees of freedom - full residual degrees of freedom).

If a difference is present between two models, means that full model, and hence the fitting of timepoint variable on the negative binomial model can

significantly and statistically explain differences based on timepoint variable. The second stage of the DEGs analysis was performed by the nbinomWaldTest function that use the default test implemented in the deseq2, the Wald test. This function tests for significance of coefficients (log_2 fold changes) in the Negative Binomial GLM, using previously calculated size factors and dispersion estimates, as stated above in the deseq2 theory paragraph. The second stage aimed to identify differentially expressed genes between acute phase (T1) and steady state phase (T3) taking into consideration the patient variable. Taking into consideration patient variable in the fitting of counts is fundamental because allow to taking into consideration the absolute patient-specific signature at ICU admission. In this way, we can force to say that DEGs between acute and recover conditions are “normalized” for patient specific variability. Conditions T1 and T3 in the second stage analysis are not characterized by the same samples as in the first-stage analysis. We indeed remove outlier samples that do not map into the main signature of T1 and T3 samples. The steps performed in the removal of these samples are described in the results chapter. P-value primary threshold for both LRT and Wald-Test was set to 0.01.

3.3.1.3 Ternary Analysis

3.3.1.3.1 Volcano plot

Volcano plot is a type of scatter-plot useful for the representation of results of -omics experiments. A volcano plot combines a measure of statistical significance from a statistical test (p value) with the magnitude of the change, enabling quick visual identification of those genes that display large magnitude changes between two conditions and that are also statistically significant. A volcano plot is constructed by plotting the negative log_{10} of the p value on the y axis and the log2foldchange between the two conditions on the x axis. This results in genes with low p values (highly significant)

appearing toward the top of the plot, whereas genes with highly positive fold change appear in the extreme right of the plot and genes with highly negative fold change in the extreme left of the plot. Volcano plots were created in R using ggplot2 package.

3.3.1.3.2 Gene Ontology analysis

Gene Ontology (GO) analysis was performed using the web tool DAVID 6.8[55] with a Gene Ontology database updated to the release of Apr 2016. DAVID website offer a Functional Annotation Tool useful to perform a GO term enrichment analysis to highlight the most relevant GO terms associated with a given gene list. The GO analysis was performed on biological processes, molecular function and cellular components. DAVID requires as input a list of genes (in our case the list of differentially expressed genes) and performs an overrepresentation analysis in order to identify in the input list GO terms including a significantly higher number of genes compared to the expected value according to the background genome. The statistical test used in DAVID is the EASE score, a modified and more conservative Fisher Exact Test. GO terms with a Benjamini adjusted p-value < 0.1 were considered significantly enriched. For each GO term the fold enrichment value, measuring the level of enrichment, was reported. With a manually curated analysis GO terms were clustered in 5 functional groups and redundant GO terms were removed.

3.3.1.3.3 Target prediction

Analysis of microRNA targets was done with TargetScan7.1 database. TargetScan predicts biological targets of miRNAs by searching for the presence of conserved 8mer, 7mer, and 6mer sites that match the seed region of each miRNA[56]. In mammals, predictions are ranked based on the predicted efficacy of targeting as calculated using cumulative weighted context++ scores of the sites[57]. As an option, predictions are also ranked

by their probability of conserved targeting[58]. TargetScanHuman considers matches to human 3' UTRs and their orthologs, as defined by UCSC whole-genome alignments.

4 RESULTS

4.1 Cohort description

A total of 32 SS patients are included in the present work. Patients have an average age of 65 years and there is a moderate prevalence of males. They are slightly overweight, with an average Body Mass Index (BMI) of 26. Mortality rate is about 30% reflecting the condition of critical illness of septic shock patients. The severity of disease was measured at ICU admission using the APACHE II score (“Acute Physiology and Chronic Health Evaluation II"). The level of organ dysfunction was assessed with the SOFA score (Sequential Organ Failure Assessment score) in order to track the patient status during the stay in the ICU [Table 1].

	Septic shock (n=32)
Age	65.91 ± 18.71
Male sex	21 (65%)
BMI	26.04 ± 5.47
APACHE II	32.65 ± 7.55
SOFA	12.55 ± 2.72
Hospital mortality (n)	10 (31%)
Mortality 28 days (n)	10 (31%)

Table 1 Clinical characteristics (mean ± stdev) of the 32 septic shock patients included in the present study.

Three main sites of infection were identified corresponding to: infections of the respiratory system, of the urinary tract and abdominal infections [Figure 9]. The infective agent was identified through blood cultures or additional sampling in the site of infection. In 14 patients a unique pathogen was identified (unimicrobial infection), whereas in 12 patients more than one infective agent was isolated (polymicrobial infection). Overall, in the cohort different kind of pathogens were identified ranging from bacteria to fungi and viral agents [Figure 9]. In 6 patients it was not possible to identify the infectious agents using microbial cultures.

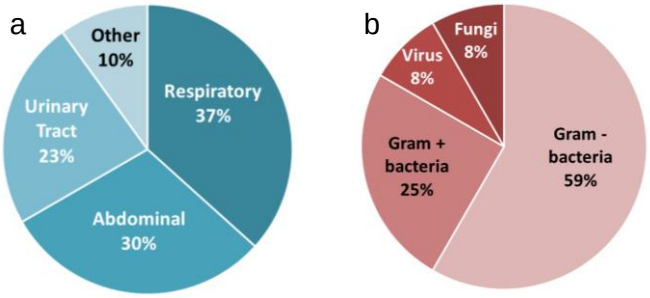

Figure 9 a) Pie chart showing the body part interested by infection b) Pie chart showing the types of infective agents identified through cultures. Data expressed in percentage referred to the 32 SS patients.

Table 2 shows the clinical characteristics of the patients at the three timepoints. A significant variation across time ($p < 0.01$) was observed for 9 clinical variables [Table 2]. As expected, septic shock is characterized by persistent hypotension, as shown by the significant decrease of systolic, diastolic and mean arterial pressure (MAP) at day 1, that tend to increase overtime. The clotting tendency of blood (prothrombin measurement) was higher at admission and it diminished later. Lactate, which is a product of the anaerobic metabolism and an important marker in shock, was detected at higher levels during the acute phase of shock (day 1) and diminished after therapies (day 3 and day 7). SOFA score showed a higher degree of organ

dysfunction at ICU admission compared to the later timepoints. Death occurred in 10 patients out of 32 at 28 days from ICU admission.

Clinical variable	Day 1	Day 3	Day 7	p-value
Systolic (mmHg)	85.18 ± 12.34	94.76 ± 14.51	111.3 ± 22.3	1.449E-05
Diastolic (mmHg)	45.18 ± 6.27	50.73 ± 8.90	55.52 ± 12.43	0.002081
MAP (mmHg)	58.18 ± 6.10	65.03 ± 8.56	73.78 ± 14.00	5.809E-06
Heart Rate (bpm)	106.4 ± 25.3	94.46 ± 23.19	102.9 ± 21.1	n.s.
Na	138.5 ± 5.7	141.2 ± 4.6	142.9 ± 5.6	n.s.
K	4.26 ± 0.87	4.06 ± 0.41	4.02 ± 0.42	n.s.
Prothrombin	1.38 ± 0.37	1.16 ± 0.23	1.11 ± 0.24	0.0004122
pH	7.29 ± 0.10	7.40 ± 0.07	7.46 ± 0.04	6.064E-08
PaO2	92.45 ± 38.52	73.46 ± 15.80	77.16 ± 20.25	n.s.
PaCO2	38.36 ± 9.99	38.46 ± 8.31	37.68 ± 8.06	n.s.
Glasgow	6.27 ± 4.42	9.84 ± 4.19	11.73 ± 4.02	0.0001084
Hematocrite	33.49 ± 5.56	30.70 ± 4.92	31.35 ± 4.55	n.s.
Leukocytes	16.85 ± 12.30	15.39 ± 9.06	13.92 ± 5.70	n.s.
Platelets	169.1 ± 103.4	158.2 ± 87.2	237.7 ± 122.3	n.s.
Creatinine	1.91 ± 1.24	1.32 ± 1.00	1.01 ± 0.59	0.0007856
Bilirubin	2.63 ± 4.91	2.32 ± 6.19	1.92 ± 4.40	n.s.
Glycemia	170.2 ± 77.0	142.8 ± 40.1	130.1 ± 34.5	n.s.
Lactate	4.90 ± 2.40	1.56 ± 0.73	1.36 ± 0.68	2.271E-10
SOFA	12.59 ± 2.68	9.57 ± 2.77	7.88 ± 3.00	2.372E-06

Table 2 Clinical characteristics of 32 septic shock patients at three timepoints (mean ± SD). P-values obtained with a Kruskal-Wallis Test. n.s. = not significant.

4.2 Transcriptomic experiment (RNAseq)

The transcriptomic dataset includes 78 biological samples collected in 32 shock patients. Gene expression profiling is available for 32 patients at day 1 (T1), for 26 patients at day 3 (T2) and for 20 patients at day 7 (T3). On average, 29.85 ± 6.74 million fragments per sample were sequenced. 64.37 ± 8.10 % of fragments mapped uniquely to the reference genome Hg38 and 48.23 ± 6.51 % million fragment counts per sample mapped uniquely and unambiguously to the Human GENCODE reference annotation file. The library preparation used in this study allows to analyze the whole transcriptome. The amount of reads produced was in line with the recommendations from the ENCODE consortium for differential expression analysis.

4.2.1 Data exploration of septic shock at three timepoints

We used Principal Component Analysis (PCA) to describe and explore the normalized gene counts dataset [Figure 10]. The PCA plot showed that biological samples are roughly clustered according to their timepoint: samples at T1 are mainly in the left part of the plot, whereas T2 samples are plotted in the central part and T3 samples in the right part of the graph. An ANOVA test on the PC1 of the three groups (T1,T2,T3) confirmed that there is a significant difference at gene expression level between the three timepoints (p-value 1.62e-10). Tukey multiple comparisons of means test showed a significant difference between each timepoint (p-value < 0.005 in each comparison).

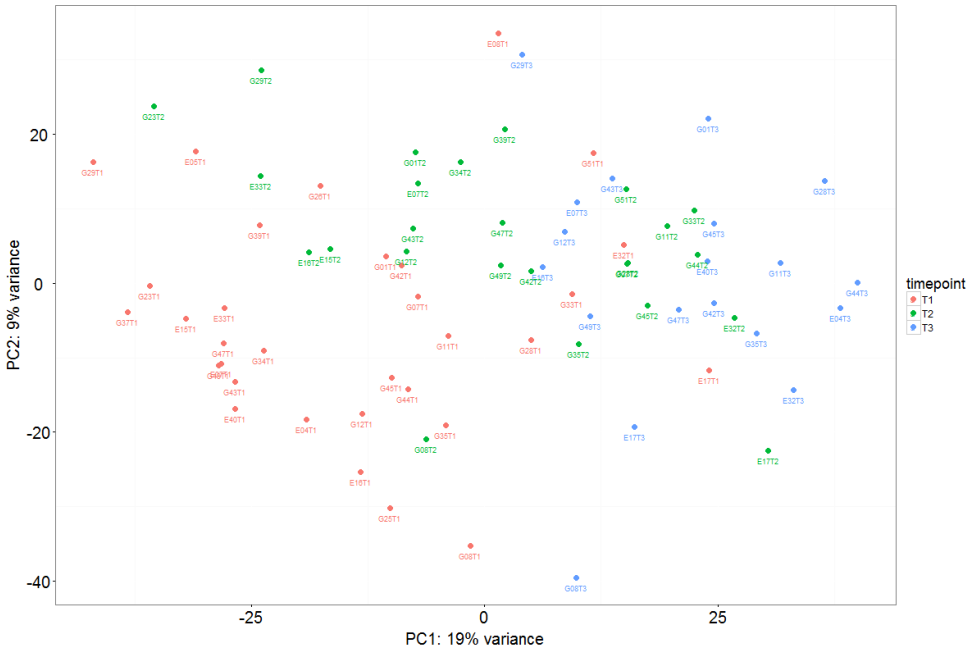

Figure 10 PCA of 32 SS patients at multiple timepoints based on the top 5000 variable genes. PC1 and PC2 of each biological sample are shown in a two-dimensional plot. Different colors are used to identify samples at different timepoints according to the legend.

A subset of the dataset including 17 patients with all three timepoints was used to perform differential expression across time. Likelyhood ratio test (LRT) (general linear model) identified 5175 transcripts showing a significant modulation of their expression across the 3 timepoints (FDR < 0.01). For downstream analysis the list of transcripts has been restricted using more stringent filtering based on expression level and statistical significance (baseMean > 20 and FDR < 0.00001). The final list included 1748 differentially expressed genes (DEGs) belonging to different categories. Gene expression data of the 1748 DEGs in the 17 patients were represented in a heat map [Figure 11]. The unsupervised hierarchical clustering identified two groups of samples in the dataset. Group A with a majority of patients at T3 (day 7) and group B with a majority of patients at T1 (day 1).The two

groups show distinct transcriptomic profiles at the 1748 genes. [Table 3]. Samples at T2, on the contrary, can be found in both branches of the condition tree showing a high inter-patient variability at this timepoint that likely reflects the individual variable response to treatment observed by clinicians. The transcriptomic profile of two patients (E17, E32) at T1 clusters in group A, showing that these patients at T1 are more similar to patients at T3. One patient (G08) had all three timepoints in group B, showing a lack of improvement of the clinical condition from T1 to T3.

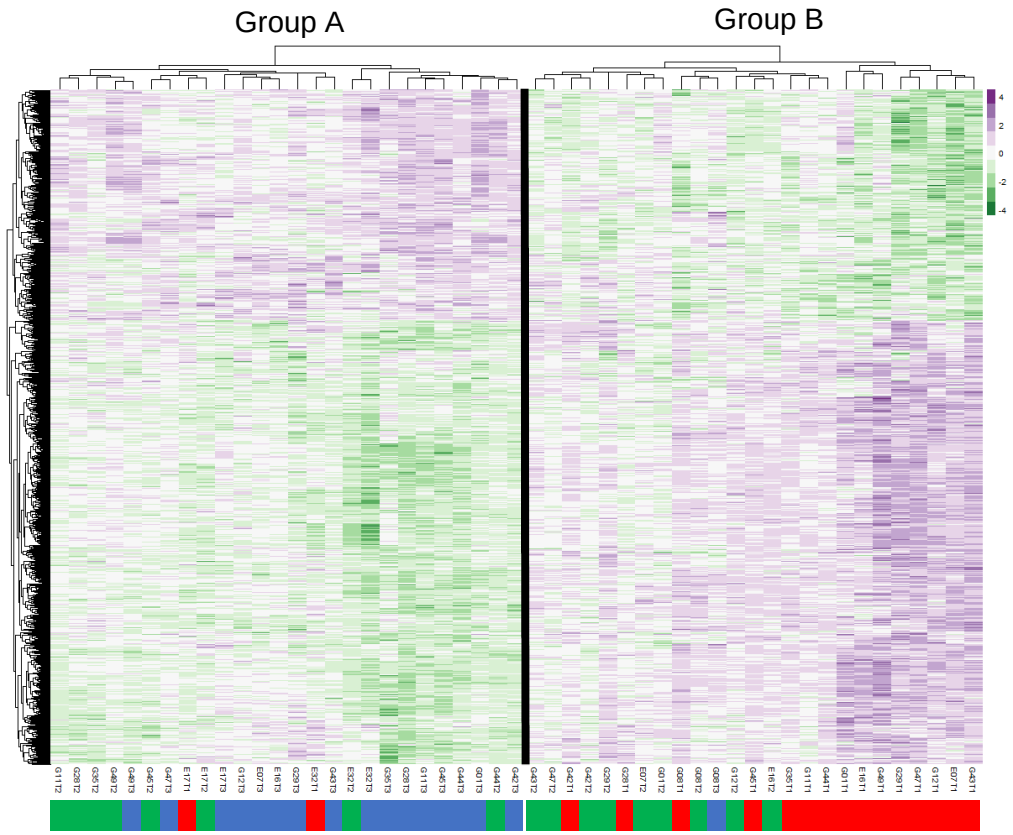

Figure 11. Unsupervised hierarchical clustering of 17 SS patients (analyzed at 3 timepoints) and 1748 genes differentially expressed during time. Clustering of genes (rows) and biological samples (columns) was based on Euclidean distance. Heatmap colors (purple and green) are based on normalized gene counts expressed in logarithmic scale. A color code was used to highlight the timepoints (red=T1, green=T2, blue=T3).

Condition	Group A (n)	Group B (n)
T1	2	15
T2	8	9
T3	16	1

Table 3 Abundance of samples in Group A and Group B according to the timepoints.

4.2.2 Data exploration of transcriptomic profiles in the whole cohort

All the available samples at condition T1 (32 patients) were clustered based on the signature composed of 1748 genes. We also included in the analysis as controls (CT), blood samples collected at day 1 from 7 septic patients who didn't develop shock.

	Septic shock (n=32)	Sepsis (n=7)	p-value
Age	65.91 ± 18.71	67.43 ± 11.46	n.s.
Male sex	21 (65%)	4 (57%)	n.s.
BMI	26.04 ± 5.47	20.83 ± 6.49	0.0386
APACHE II	32.65 ± 7.55	21.57 ± 4.50	0.0009
SOFA	12.55 ± 2.72	9.29 ± 3.09	0.0184
Hospital mortality	10 (31%)	0 (0%)	n.s.
Mortality 28 days	10 (31%)	0 (0%)	n.s.

Table 4 Clinical characteristics of septic shock patients compared to sepsis patients used as controls (mean ± SD). P-values obtained with a Wilcoxon Rank Sum Test. n.s. = not significant.

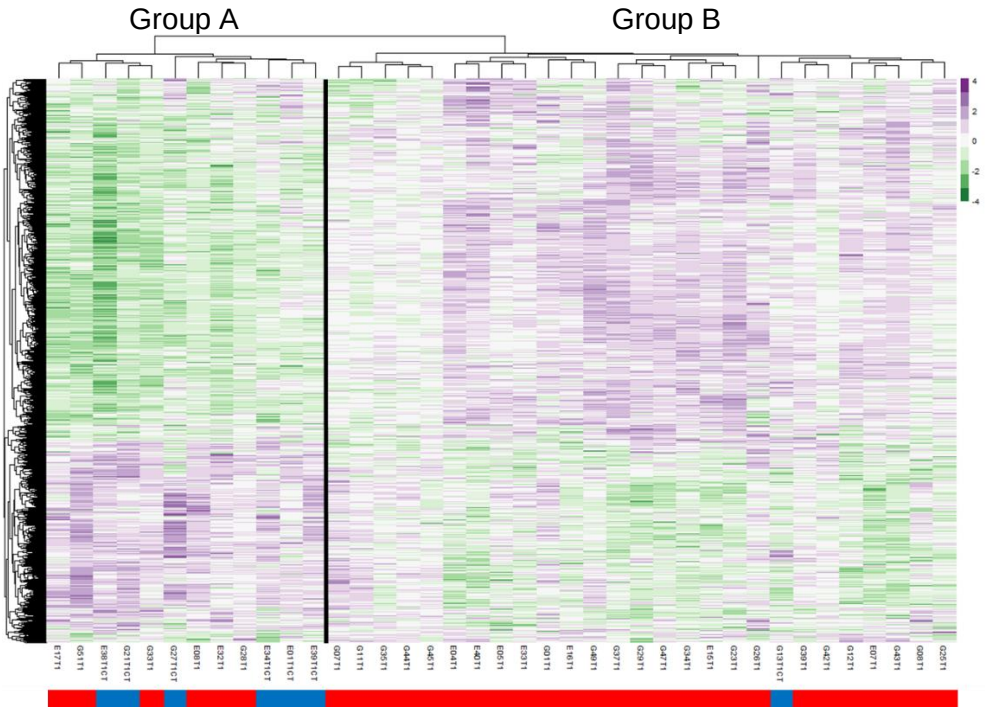

Figure 12 Unsupervised hierarchical clustering of 32 septic shock patients and 7 septic controls at day 1 with a selection of 1748 genes. A color code was used to highlight SS patients and septic controls (red=Septic shock, blue=Septic control).

The dendrogram divides the dataset in two groups. Branch A contains 12 patients (6 sepsis controls and 6 SS patients). Branch B contains 26 septic shock patients and 1 septic control. Septic shock patients in group A show an expression pattern similar to septic controls and different from the other septic shock patients, showing that a wide variability can be observed at the molecular level among septic shock patients.

Condition	Group A	Group B
Septic shock	6	26
Sepsis control (CT)	6	1

Table 5 Abundance of samples in Group A and Group B according to the condition.

4.2.3 Differential expression analysis: acute phase vs steady state

The analysis of gene expression across three timepoints discussed above has identified timepoints T1 and T3 as the most significantly different both on a clinical and on a molecular basis. We then performed an additional analysis comparing gene expression between T1 and T3 in order to highlight the genes modified during the transition from the acute phase of shock to the steady state. Moreover, based on the heatmaps [Figure 11, Figure 12] we decided to discard 4 SS patients (E17, E32, G28 and G08) because the clusterization of their timepoints was different from that of the majority of patients. Principal Component Analysis (PCA) shows that patients selected for analysis at T1 and T3, are completely separated based on the first principal component [Figure 13].

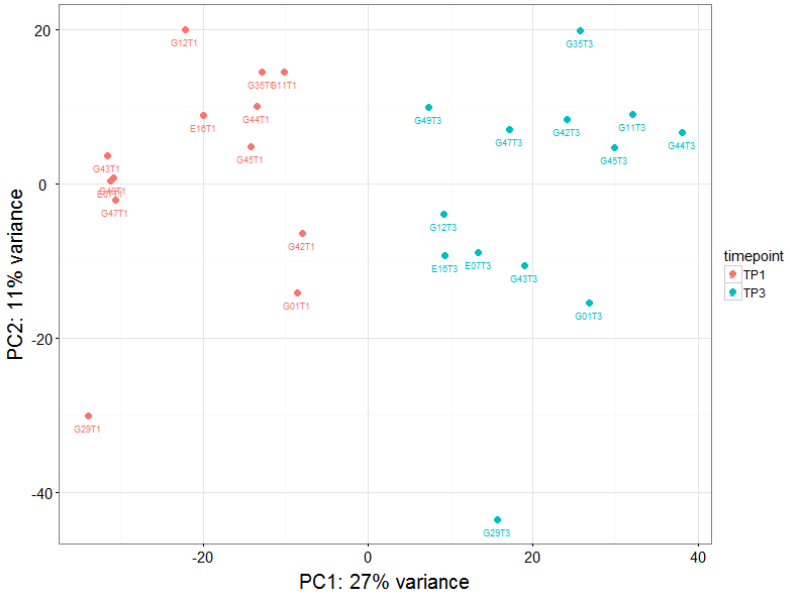

Figure 13 PCA analysis on the 5000 most variable genes in a dataset of 13 septic shock patients. PC1 and PC2 of each biological sample are shown in a two-dimensional plot. Different colors are used to identify samples at different timepoints according to the legend.

Septic shock patients analyzed at T1 and T3 (n=13)	
Age	63.07 ± 21.48
Male sex	10 (76.92%)
BMI	27.82 ± 6.41
APACHE II	32.38 ± 9.30
SOFA T1	12.15 ± 1.95
SOFA T3	7.33 ± 2.38
Hospital mortality (n)	2 (15.38%)
Mortality 28 days (n)	2 (15.38%)

Table 6 Clinical characteristics of 13 septic shock patients analyzed in the acute phase and the steady state of shock (mean ± SD).

As shown in Table 6, the 13 patients analyzed were homogeneous for two parameters (APACHE II and SOFA T1) that characterized the shock condition at admission and for SOFA at T3. The majority of the patients are males and mortality affected 2 patients out of 13. The age was heterogeneous including patients from 25 to 86 years.

Differential expression analysis identified 4842 genes modulated between T1 and T3 (FDR < 0.01). For downstream analysis the list of transcripts has been narrowed using more stringent filtering based on expression level and statistical significance (baseMean > 20 and (FDR < 0.00001 or |logFC| >1)). We reduced the list to 1981 DEGs with 789 upregulated and 1192 downregulated genes [Figure 14, Table 7].

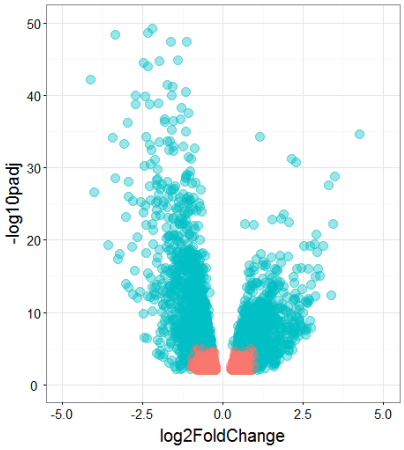

Figure 14 Volcano plot of the comparison between T1 and T3. The plot shows fold change and FDR in logarithmic scale of 4842 differentially expressed genes. Blue color identifies 1981 DEGs passing the filter of log_2FC and FDR values.

Transcript category	Abundance
protein coding	1791
lincRNA	37
antisense RNA	38
pseudogene	30
other RNAs	85

Table 7 Description of differentially expressed genes between day 1 and day 7 based on the transcript category.

4.2.4 Pathway analysis

The list with 1981 differentially expressed genes (DEGs) has been analyzed with DAVID 6.8 functional annotation tool to identify overrepresented biological processes, molecular functions and cellular components. Significant ontology terms were selected using a p-value threshold (Benjamini adjusted p-value < 0.1) and they were clustered in functional macro groups with a curated procedure [Table 8][Appendix:Table 13,Table 14]. The groups identified are related to the functions of the immune systems, inflammation, innate and adaptive immune response. A group of ontology terms related to protein synthesis and transport of vesicles was also identified [Figure 15].

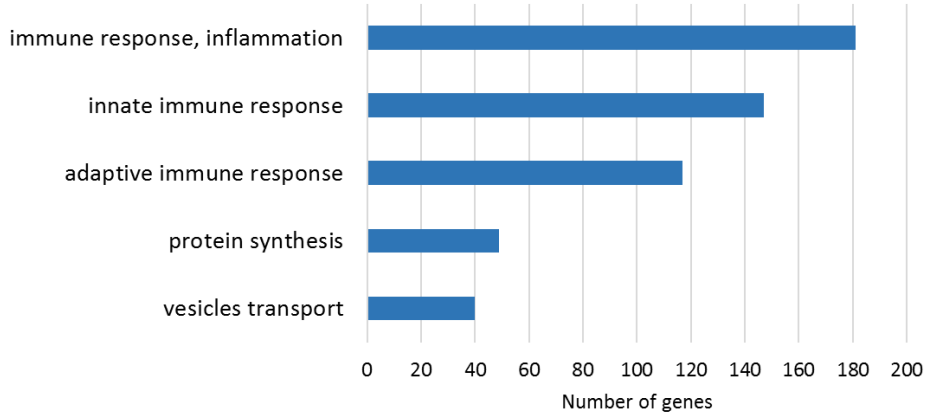

Figure 15 Bar plot showing the number of differentially expressed genes in each ontology macro group. Counts are referred to genes belonging to GO terms of the category of Biological Processes (BP).

Biological group	Gene Ontology	Category	Genes	Fold Enrichment	Adjusted p-value
Innate immune response	GO:0038096:Fc-gamma receptor signaling pathway involved in phagocytosis	BP	41	3.84	1.48E-10
	GO:0038095:Fc-epsilon receptor signaling pathway	BP	43	2.73	1.65E-06
	GO:0045087:innate immune response	BP	83	1.92	4.83E-06
	GO:0042742:defense response to bacterium	BP	35	2.35	1.19E-03
	GO:0002755:MyD88-dependent toll-like receptor signaling pathway	BP	12	3.64	3.24E-02
	GO:0002223:stimulatory C-type lectin receptor signaling pathway	BP	24	2.29	3.31E-02
Adaptive immune response	GO:0002250:adaptive immune response	BP	44	3.04	6.97E-08
	GO:0050853:B cell receptor signaling pathway	BP	25	4.64	9.54E-08
	GO:0050852:T cell receptor signaling pathway	BP	41	2.76	2.50E-06
	GO:0050871:positive regulation of B cell activation	BP	14	5.39	1.36E-04
	GO:0031295:T cell costimulation	BP	20	2.57	2.85E-02
	GO:0042110:T cell activation	BP	14	3.05	5.34E-02
	GO:0030217:T cell differentiation	BP	11	3.67	5.65E-02
Immune response, inflammation	GO:0006955:immune response	BP	84	2.00	7.67E-07
	GO:0050776:regulation of immune response	BP	44	2.77	8.92E-07
	GO:0007249:I-kappaB kinase/NF-kappaB signaling	BP	19	3.17	4.12E-03
	GO:0006954:inflammatory response	BP	63	1.65	1.70E-02
	GO:0050900:leukocyte migration	BP	27	2.20	2.72E-02
	GO:0000502:proteasome complex	CC	15	2.56	4.53E-02
	GO:0004175:endopeptidase activity	MF	15	2.80	7.22E-02
Vesicles	GO:0070062:extracellular exosome	CC	416	1.55	4.27E-20
	GO:0006888:ER to Golgi vesicle-mediated transport	BP	33	2.07	1.83E-02
	GO:0048208:COPII vesicle coating	BP	17	2.79	3.22E-02
	GO:0072562:blood microparticle	CC	27	1.94	4.21E-02
Protein synthesis	GO:0006614:SRP-dependent cotranslational protein targeting to membrane	BP	28	2.92	1.95E-04
	GO:0006364:rRNA processing	BP	43	1.98	5.15E-03
	GO:0015935:small ribosomal subunit	CC	11	4.24	5.93E-03
	GO:0022625:cytosolic large ribosomal subunit	CC	16	2.38	6.00E-02
	GO:0006413:translational initiation	BP	28	2.02	6.37E-02
	GO:0003735:structural constituent of ribosome	MF	39	1.75	7.67E-02

Table 8 Gene Ontology analysis results. The table reports enriched GO terms (BP, MF, CC) with a p-adjusted value > 0.1 (Benjamini correction). GO terms have been grouped in 5 main groups with a curated analysis. For each GO term the following information are reported: the category (BP = Biological Process, MF = Molecular Function, CC = Cellular Component), the number of genes, the Fold Enrichment compared to the expected number of genes in the human genome, the Benjamini adjusted p-value resulting from the modified Fisher Exact test (EASE score).

4.2.4.1 Pathways of the innate immune response

At day 7, it was observed the downregulation of pathways involved in the recognition of pathogens such as Toll-like receptor and C-type lectin receptor signaling pathways [Figure 16]. Downregulation involves receptors TLR1, TLR2, TLR4, TLR5, TLR8 as well as the protein kinase IRAK4 necessary in the downstream signaling leading to the transcriptional activation of inflammatory genes. On the contrary upregulation of TLR7 is observed. The c-type lectin receptors CLEC4D, CLEC6A (alias Dectin2), CLEC4E (alias Mincle) are downregulated as well as the adaptor molecule FCER1G (Fc Receptor Gamma-Chain) and the tyrosine kinase SYK acting in the downstream signaling pathways that modulate cytokine expression. Pathways involving recognition of antigens bound to immunoglobulins IgE and IgG are also modified.

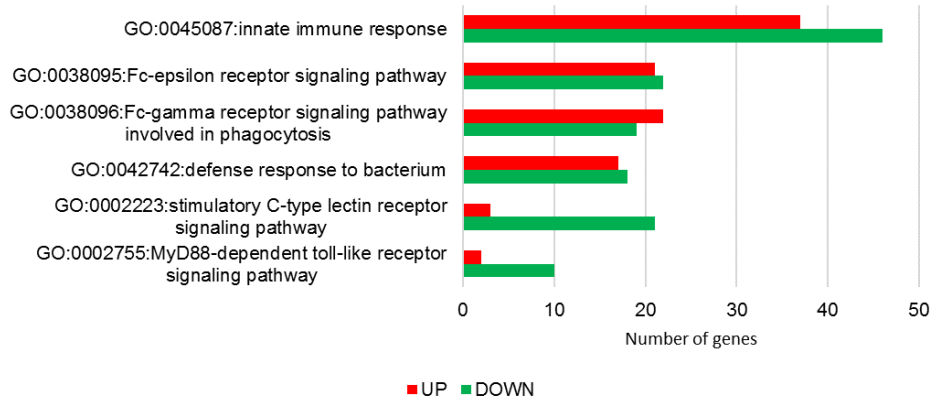

Figure 16 Bar plot showing the number of upregulated genes (red) and downregulated genes (green) at day 7 compared to day 1. GO terms in the cluster of innate immune response are reported.

4.2.4.2 Pathways of immune response and inflammation

A regulation of the inflammatory pathway is observed at day 7: receptors of the powerful proinflammatory cytokines IL1 and IL18 (respectively IL1R2, IL1RAP and IL18R1 and IL18RAP), are downregulated. The alarmins S100A8, S100A9, S100A12 which have a proinflammatory activity are downregulated as well as the genes of the proteasome and genes of NFKB signaling pathway [Figure 17].

Prostaglandin-endoperoxide synthase (PTGS2), the key enzyme in prostaglandin biosynthesis is upregulated as well as ALOX15, a lipoxygenase converting arachidonic acid and generating a spectrum of bioactive lipid mediators. On the contrary PTGER2 and LTB4R that are respectively receptors for prostaglandins and leukotrienes, inflammatory lipids derived from arachidonic acid, are downregulated. Upregulation is observed also for CHI3L1, a carbohydrate-binding lectin, playing a role in the process of inflammation and tissue remodeling and OLR1, a receptor that mediates the recognition, internalization and degradation of oxidatively modified low density lipoprotein (oxLDL).

Molecules with endopeptidase activity potentially involved in the inflammatory and remodeling processes of the extracellular matrix are also dysregulated: the metalloproteases ADAMTS3, MMP8 and MMP9 are downregulated at day 7 whereas HtrA serine peptidase (HTRA3), Neutrophil Elastase (ELANE) and the metalloendopeptidase Neprilysin (MME) are upregulated at the same timepoint. Genes involved in cell adhesion and leukocyte migration are also regulated: at day 7 the expression of CD177, CD44, and CEACAM1 is decreased whereas the expression of CEACAM6 and CEACAM8 is increased.

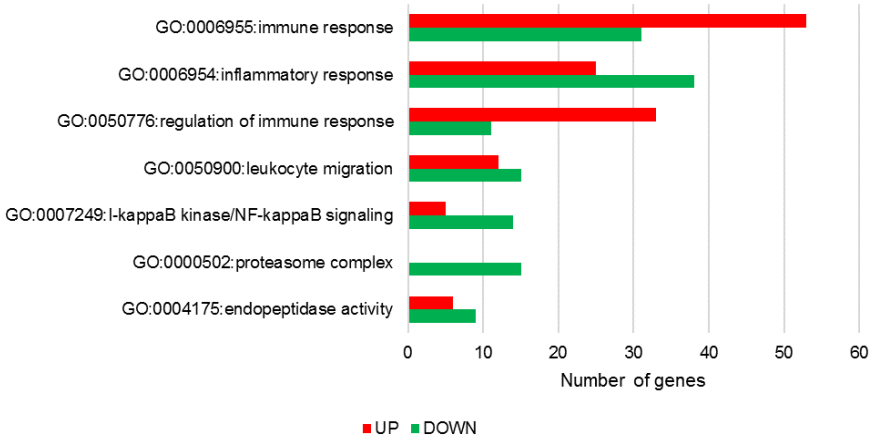

Figure 17 Bar plot showing the number of upregulated genes (red) and downregulated genes (green) at day 7 compared to day 1. GO terms in the cluster of immune response and inflammation are reported.

4.2.4.3 Pathways of adaptive immune response: T and B lymphocytes

At steady state (Day 7), genes involved in T cell activity are upregulated: CD4 receptor (T helper) that interacts with the major histocompatibility complex class II antigens, CD8A and CD8B receptors in cytotoxic T cells recognizing antigens displayed by antigen presenting cell (APC) in the context of class I MHC molecules. Genes involved in T cell costimulation also increase their expression: CD28 and CD26 (alias DPP4) expressed on T lymphocytes and CD86 expressed on APCs. Upregulation is reported also for genes with adaptor function in the T cell receptor signaling (TRAT1 and LAX1) and for kinases involved in the initial step of TCR-mediated signal transduction (ZAP70 and LCK).

Genes involved in B cell activation encoding the heavy chain (IGHG1, IGHV3-23, IGHG3, IGHA2, IGHA1, IGHG4, IGHG2), and the light chain of immunoglobulins (IGKC, IGLC3, IGLC2) are upregulated at day 7 [Figure 18].

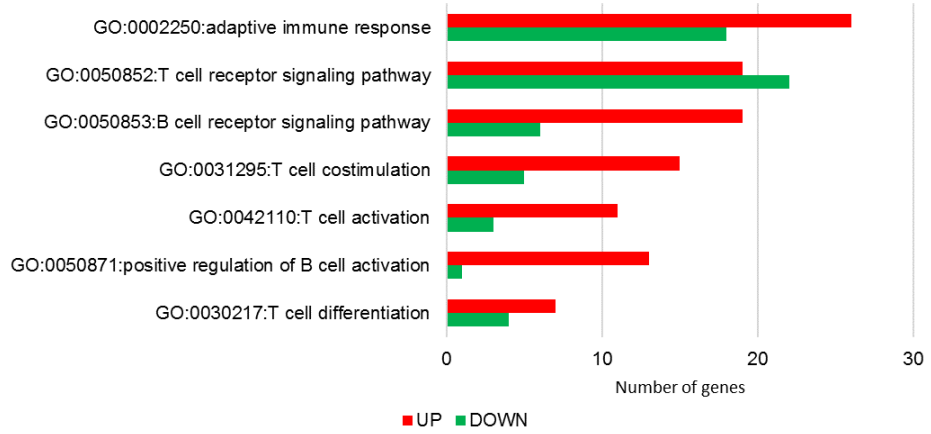

Figure 18 Bar plot showing the number of upregulated genes (red) and downregulated genes (green) at day 7 compared to day 1. GO terms in the cluster of adaptive immune response are reported.

4.2.4.4 Vesicles

A regulation of genes involved in vesicle transport between endoplasmic reticulum and Golgi apparatus was observed, particularly related to COPII coated vesicles. Enrichment in genes related to extracellular exosomes and blood microparticles is also found [Figure 19]. These genes were downregulated at day 7, suggesting their role in the acute phase T1.

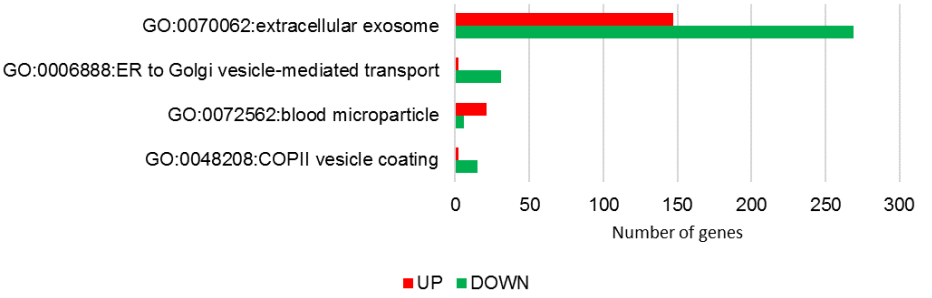

Figure 19 Bar plot showing the number of upregulated genes (red) and downregulated genes (green) at day 7 compared to day 1. GO terms in the cluster of vesicles processes are reported.

4.2.4.5 Protein synthesis

Increased expression was observed for genes related to protein synthesis. Genes encoding constituents of small and large ribosomal subunits and involved in rRNA processing are upregulated at day 7 [Figure 20]. Differential expression was observed for genes involved in translational initiation (EIF3L, EIF4E3).

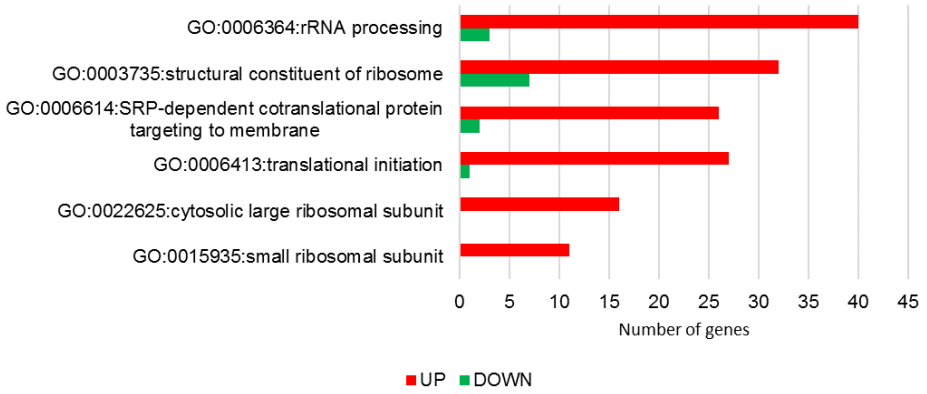

Figure 20 Bar plot showing the number of upregulated genes (red) and downregulated genes (green) at day 7 compared to day 1. GO terms in the cluster of protein synthesis are reported.

4.2.5 Analysis of top differentially expressed genes

In order to identify the most involved molecular functions in the transition from the acute phase of shock to the steady state, we selected the top upregulated or downregulated genes applying a threshold on the log2FoldChange value. Up or down regulation always refer to T3 compared to T1. A total of 149 genes with a log2FoldChange > 2 or < -2 were identified and their molecular functions were analyzed using a curated approach. Sixty three genes were associated to common biological processes or molecular functions [Table 9]. With this approach we observed a strong upregulation of 27 genes encoding the heavy and light chains of immunoglobulins. Among the genes related to immune functions and inflammation, downregulation was observed for receptors of the IL-1 family, the alarmin S100A12 and for CD163, a receptor involved in the acute phase of inflammation, exclusively expressed in monocytes and macrophages In the same biological group on the contrary, galectin 2 and chitinase 3 like 1, involved in inflammation and tissue remodeling were upregulated. Molecules of the class of lipid mediators, that are known as key players in the resolution of inflammation and in the return to homeostasis, were either up or down regulated in the steady state. The lipid receptors FFAR3, S1PR1 and FABP2 and two genes involved in the metabolism of prostaglandins and leukotrienes (HPGD and ALOX15B) were downregulated. OLR1, the receptor of oxidized LDL, ALOX15, the arachidonate 15-lipoxygenase, PTGDR2, a prostaglandin receptor, and SCARF1, involved in the clearance of apoptotic cells were upregulated. Four genes involved in carbohydrate metabolism showed lower expression at steady state condition. Upregulation was observed for CAMP, DEFA3 and DEFA4 encoding peptides with antimicrobial functions and myeloperoxidase producing hypohalous acids with microbicidal activity.

Genes encoding proteases involved in antimicrobial functions, inflammation and tissue remodeling were also markedly downregulated and upregulated.

Biological group	Gene_ID	log2FC	Description
Immune functions and inflammation	IL1R2	-3.08	interleukin 1 receptor type 2
	CD163	-2.81	CD163 molecule
	CD163L1	-2.68	CD163 molecule like 1
	IL18R1	-2.43	interleukin 18 receptor 1
	S100A12	-2.27	S100 calcium binding protein A12
	IL18RAP	-2.24	interleukin 18 receptor accessory protein
	IL1RAP	-2.06	interleukin 1 receptor accessory protein
	LGALS2	2.15	galectin 2
	CHI3L1	2.52	chitinase 3 like 1
Lipid mediators	HPGD	-3.57	hydroxyprostaglandin dehydrogenase 15-(NAD)
	FFAR3	-3.36	free fatty acid receptor 3
	ALOX15B	-2.59	arachidonate 15-lipoxygenase, type B
	S1PR1	-2.13	sphingosine-1-phosphate receptor 1
	FABP2	-2.06	fatty acid binding protein 2
	SCARF1	2.23	scavenger receptor class F member 1
	PTGDR2	2.26	prostaglandin D2 receptor 2
	ALOX15	2.71	arachidonate 15-lipoxygenase
	OLR1	2.75	oxidized low density lipoprotein receptor 1
Carbohydrate metabolism	PFKFB2	-3.34	6-phosphofructo-2-kinase/fructose-2,6-biphosphatase 2
	IDNK	-2.40	IDNK, gluconokinase
	PFKFB3	-2.21	6-phosphofructo-2-kinase/fructose-2,6-biphosphatase 3
	HK3	-2.11	hexokinase 3
Protease activity	PCSK9	-2.94	proprotein convertase subtilisin/kexin type 9
	ADAMTS3	-2.93	ADAM metallopeptidase with thrombospondin type 1 motif 3
	HGF	-2.71	hepatocyte growth factor
	HTRA3	2.06	HtrA serine peptidase 3
	PRTN3	2.34	proteinase 3
	ELANE	2.43	elastase, neutrophil expressed
	MME	2.47	membrane metallo-endopeptidase
	PLAU	2.51	plasminogen activator, urokinase
	AZU1	2.94	azurocidin 1
	CTSG	3.48	cathepsin G
Antimicrobial activity	MPO	2.21	myeloperoxidase
	CAMP	2.58	cathelicidin antimicrobial peptide
	DEFA3	3.02	defensin alpha 3
	DEFA4	3.44	defensin alpha 4
Immunoglobulin	IGKC	2.04	immunoglobulin kappa constant
	IGHV3-7	2.05	immunoglobulin heavy variable 3-7
	IGLC3	2.06	immunoglobulin lambda constant 3 (Kern-Oz+ marker)
	IGKV1-5	2.06	immunoglobulin kappa variable 1-5
	IGLV2-11	2.06	immunoglobulin lambda variable 2-11
	IGHV3-23	2.11	immunoglobulin heavy variable 3-23
	IGHG3	2.12	immunoglobulin heavy constant gamma 3 (G3m marker)
	IGKV1-6	2.15	immunoglobulin kappa variable 1-6
	IGLC2	2.17	immunoglobulin lambda constant 2
	IGHA2	2.20	immunoglobulin heavy constant alpha 2 (A2m marker)
	IGKV3-20	2.22	immunoglobulin kappa variable 3-20
	IGLV1-47	2.26	immunoglobulin lambda variable 1-47
	IGLV2-8	2.26	immunoglobulin lambda variable 2-8
	IGKV1-12	2.29	immunoglobulin kappa variable 1-12
	IGHA1	2.33	immunoglobulin heavy constant alpha 1
	IGLV2-23	2.36	immunoglobulin lambda variable 2-23
	IGKV2-24	2.38	immunoglobulin kappa variable 2-24
	IGLV6-57	2.39	immunoglobulin lambda variable 6-57
	IGKV4-1	2.39	immunoglobulin kappa variable 4-1
	IGKV1-17	2.39	immunoglobulin kappa variable 1-17
	IGHV3-74	2.42	immunoglobulin heavy variable 3-74
	IGLV7-43	2.57	immunoglobulin lambda variable 7-43
	IGLV7-46	2.62	immunoglobulin lambda variable 7-46 (gene/pseudogene)
	IGLV8-61	2.63	immunoglobulin lambda variable 8-61
	IGHV3-15	2.69	immunoglobulin heavy variable 3-15
	IGHG4	2.75	immunoglobulin heavy constant gamma 4 (G4m marker)
	IGHG2	3.37	immunoglobulin heavy constant gamma 2 (G2m marker)

Table 9 Functional analysis of top differentially expressed genes. Sixty three genes showing high fold-induction were clustered in 6 biological groups based on their function.

4.2.6 Analysis of long non coding RNAs

The expression of long non coding RNAs (lncRNAs) was analyzed in order to identify transcripts associated to septic shock condition, potentially useful as biomarkers. A total of 30 lncRNAs differentially expressed between the acute phase of septic shock and the steady state, were identified after applying a fold change threshold (log_2FC >1 or < -1) [Table 11]. The lncRNA with the highest level of significance is LINC01127. It is located on chr 2 upstream the IL1R2 gene and other interleukin receptors of the IL1 family of cytokines (IL1R1, IL1RL2, IL18R1, IL1RL1, IL18RAP). Four of the cited interleukin receptors are downregulated in our experiment showing coexpression with LINC01127 [Table 10]. In this region is also located MIR4772, a microRNA previously associated to sepsis. Downregulation was also observed for MIAT, a lncRNA previously associated to myocardial infarction and cardiac hypertrophy.

Gene_ID	log_2FC	FDR	description
LINC01127	**-1.63**	2.0E-19	long intergenic non-protein coding RNA 1127
IL1R2	**-3.08**	4.9E-34	interleukin 1 receptor type 2
IL18R1	**-2.43**	1.8E-25	interleukin 18 receptor 1
IL1RL1	**-0.93**	7.8E-06	interleukin 1 receptor like 1
IL18RAP	**-2.24**	3.6E-33	interleukin 18 receptor accessory protein

Table 10 LINC01127 is coordinately downregulated with downstream located genes encoding interleukin receptors. Log_2FC is log_2FoldChange of Day 7 expression compared to day 1. FDR stands for False Discovery Rate.

Ensembl Gene ID	Gene ID	log_2FC	FDR
ENSG00000281162	LINC01127	-1.63	2.01E-19
ENSG00000245937	LINC01184	1.22	3.32E-17
ENSG00000253214	RP11-1149M10.2	-1.62	3.5E-16
ENSG00000268734	CTB-61M7.2	-1.64	2.89E-14
ENSG00000262370	RP11-473M20.9	1.38	1.62E-13
ENSG00000229647	AC007879.7	-1.95	2.32E-13
ENSG00000226328	NUP50-AS1	1.46	4.36E-13
ENSG00000254789	RP11-531H8.2	2.63	5.55E-12
ENSG00000267194	RP1-193H18.2	-1.37	3.03E-11
ENSG00000235192	AC009495.2	-1.31	1.22E-10
ENSG00000248323	LUCAT1	1.71	1.54E-09
ENSG00000262714	RP11-44F14.8	1.81	2.03E-09
ENSG00000261804	RP11-44F14.2	1.67	5.32E-09
ENSG00000245164	LINC00861	1.59	8.91E-09
ENSG00000258476	RP11-76E17.3	-1.42	3.34E-08
ENSG00000255328	RP11-326C3.12	-1.21	6.11E-08
ENSG00000225783	MIAT	-1.36	4.17E-07
ENSG00000203709	C1orf132	1.09	3.04E-06
ENSG00000256039	RP11-291B21.2	1.40	3.96E-06
ENSG00000248455	RP11-321E2.3	-1.20	7.52E-06
ENSG00000270972	RP11-326C3.15	-1.11	1.06E-05
ENSG00000271204	RP11-138A9.1	1.29	1.11E-05
ENSG00000251230	MIR3945HG	-1.37	1.65E-05
ENSG00000249173	LINC01093	-1.96	1.8E-05
ENSG00000230839	RP5-968J1.1	-1.09	2.47E-05
ENSG00000231551	RP11-495P10.1	-1.02	3.31E-05
ENSG00000255801	RP11-561P12.5	1.33	9.27E-05
ENSG00000226380	MIR29A	1.11	0.000205
ENSG00000254006	RP11-1D12.2	1.20	0.002441
ENSG00000259959	RP11-121C2.2	1.08	0.002767

Table 11 List of thirty differentially expressed long non coding RNAs between the acute phase and steady state of septic shock. Log_2FC is log_2FoldChange of Day 7 expression compared to day 1. FDR stands for False Discovery Rate.

4.3 microRNA analysis

The miRNA dataset includes 75 biological samples collected from 32 shock patients. Gene expression profiling is available for 32 patients at day 1 (T1), for 25 patients at day 3 (T2) and for 18 patients at day 7 (T3). On average, 7 M reads per sample were produced, that represent an adequate number of reads to capture a meaningful fraction of miRNA present in the samples. Principal Component Analysis (PCA) was used to analyze normalized gene counts [Figure 21].

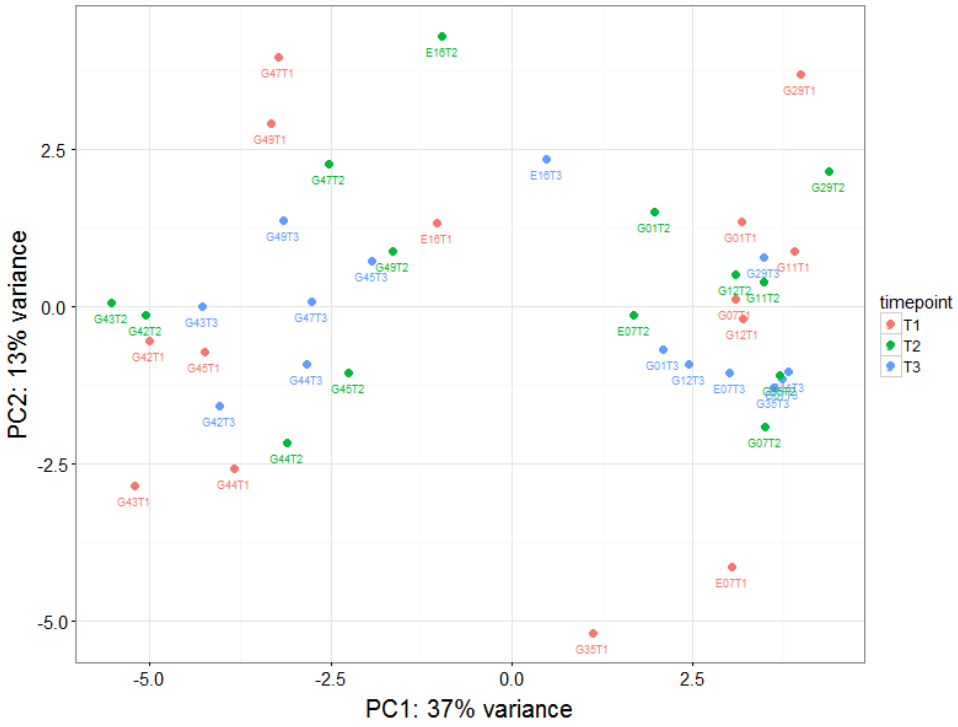

Figure 21 PCA of 14 SS patients at multiple timepoints based on the top 50 variable miRNAs. PC1 and PC2 of each biological sample are shown in a two-dimensional plot. Different colors are used to identify samples at different timepoints according to the legend.

Contrary to what we observed in the PCA plot of gene expression data [Figure 10], in the PCA plot of microRNA data we couldn't observe a clusterization of biological samples based on timepoints. Instead, microRNA expression shows a high inter-patient variability. Given this high variability, we decided to analyze a subgroup of patients, as homogeneous as possible. Patients were selected based on the same criteria used for RNASeq analysis: we focused on the condition of acute phase of shock (Day 1) and the condition of steady state (Day 7); 4 SS patients (E17, E32, G28 and G08) were excluded from the dataset because in the clustering analysis of RNASeq their gene expression profile was different compared to most of the other samples in the dataset. Based on this, 14 patients were selected to investigate microRNA expression. Eight differentially expressed microRNAs were identified after applying filters based on average number of sequences covering each miRNA, p value of significance of the difference, logFC of the difference (basemean > 10, significance level of 0.05, logFC > 0.5) (Table 12).

microRNA_ID	**log_2FoldChange**	**FDR**
hsa-miR-125a-5p	**1.57**	5.60E-10
hsa-miR-150-5p	**1.18**	4.47E-06
hsa-miR-99b-5p	**0.93**	0.003
hsa-miR-193a-3p	**-1.33**	0.012
hsa-miR-199b-5p	**-0.77**	0.015
hsa-miR-26b-3p	**-0.78**	0.015
hsa-miR-27a-3p	**-0.63**	0.017
hsa-miR-96-5p	**-0.66**	0.018

Table 12 List of differentially expressed microRNAs between the acute phase and steady state of septic shock. Log_2FC is log_2FoldChange of Day 7 expression compared to day 1. FDR stands for False Discovery Rate.

The expression of the top 2 upregulated and of the top downregulated miRNA are shown with expression boxplots [Figure 22, Figure 23].

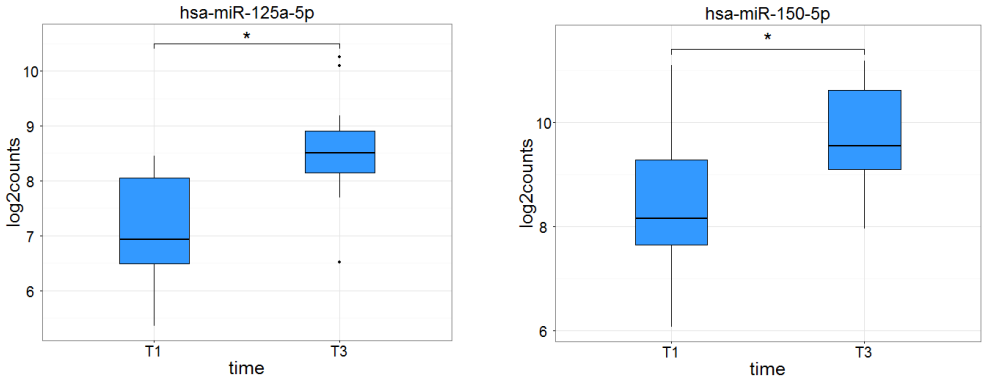

Figure 22 Expression boxplots of microRNAs 125a-5p and 150-5p showing upregulation in the steady state of septic shock (T3) compared to the acute phase of shock (T1).

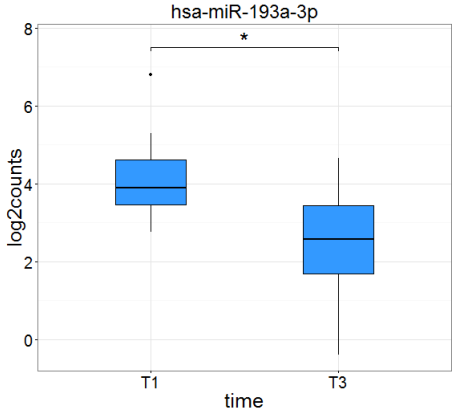

Figure 23 Expression boxplot of microRNA 193a-3p showing its downregulation in the steady state of septic shock (T3) compared to the acute phase of shock (T1).

4.3.1 "In silico" target prediction

Three microRNAs showing high expression fold change (log_2FoldChange >1 or < -1) were selected in order to identify their putative targets: the top2 upregulated hsa-miR-125a-5p and hsa-miR-150-5p, and the downregulated hsa-miR-193a-3p. At this purpose we used TargetScan 7.1 database and identified 946 target genes for miR-125a-5p, 439 targets for miR-150-5p and 340 targets for miR-193a-3p.

4.3.1.1 Targets of upregulated miRNAs miR-125a-5p and miR-150-5p

Since miR-125a-5p and miR-150-5p are both upregulated, the lists of their targets were merged, generating a list of 1329 target genes. As expected, the number of targets of the two miRNA is very high and unlikely to be used for any further investigation. Therefore, being the two miRNA upregulated, we searched, in the list of genes downregulated in the RNAseq experiment, for those genes that are targets of miR-125 and miR-150. In this way we could restrict the list to 193 genes [Figure 24] showing downregulation in the RNASeq experiment. This shortened list was used for a more in depth downstream analysis. An overrepresentation analysis of these 193 genes identified a significant GO enrichment for the pathway "hsa04010:MAPK signaling" with a Benjamini adjusted p-value of 0.015. Eleven genes in MAP Kinase pathway are downregulated in the RNAseq experiment and are targets of miR125a-5p and/or miR150-5p (DUSP3, RPS6KA1, TAOK1, MAPK14, TGFBR1, MAP3K1, MAPK10, TRAF6, SRF, MAP2K6, RASA2). MAPK10 and MAPK14 are also known with the name of JNK3 and p38 that are important regulatory molecules in the MAPK pathway.

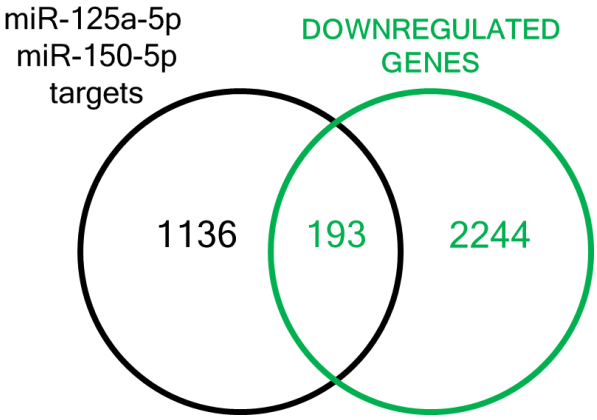

Figure 24 Venn diagram showing the filtering procedure applied to the list of target genes obtained from TargetScan database. The list of 1329 targets was intersected with the list of 2437 downregulated genes in the RNASeq experiment (FDR < 0.01) considering the same comparison (Day1 – Day7). A total of 193 genes defined as targets of miR125a-5p or miR150-5p were downregulated in our dataset.

4.3.1.2 Targets of the downregulated miRNA miR-193a-3p

We identified 340 targets for miR-193a-3p, that is downregulated at T3. With the aim to circumscribe the list of target genes, we concentrated on targets that were upregulated genes in RNAseq experiment. In this way we reduced the number to 38 targets [Figure 25].

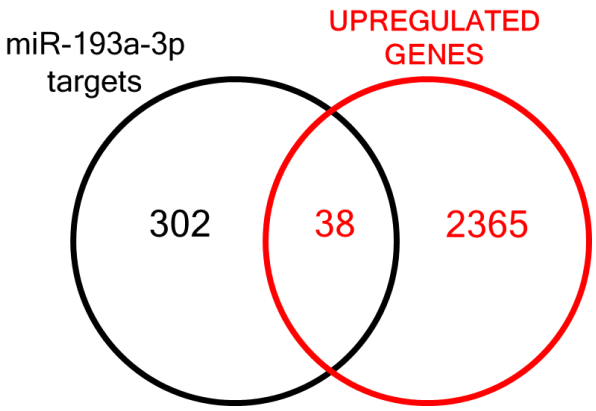

Figure 25 Venn diagram showing the filtering procedure applied to the list of target genes obtained from TargetScan database. The list of 340 targets was intersected with the list of 2403 upregulated genes in the RNASeq experiment (FDR < 0.01) considering the same comparison (Day1 – Day7). A total of 38 genes defined as targets of miR-193a-3p were upregulated in our dataset.

Gene Ontology overrepresentation analysis didn't identify any significative GO enrichment in the list of 38 upregulated targets. Nevertheless we were able to observe the presence of 3 genes involved in the response to hypoxia: ETS1, PLAU and TGFBR3.

5 DISCUSSION

We analyzed the transcriptomic profile of septic shock patients at three critical points of the clinical course, to investigate the molecular mechanisms involved, in relation to the clinical condition. The experimental design of this study includes a follow up of the patients during the ICU stay, from admission up to 7 days of the ICU stay [59]. This represents an important asset that can help to pinpoint genes and molecular pathways that are at work during the period of observation. As far as we know this is the first transcriptomic study in septic shock patients with a follow up of 7 days. In fact, most papers published so far that have profiled the transcriptome in septic shock have evaluated patients at the time of their admission to the ICU[60]–[62] or in the early phase after ICU admission [63]. We performed the RNAseq experiments in peripheral blood cells, that are the first line of immune defense system and continuously interact with the other tissues and organs of the body. In circulating blood cells the expression of a large proportion of the genes encoded in human genome can be detected. It has been demonstrated that these cells can be used as surrogate tissue since changes of their gene expression can provide useful information on health or disease condition of any tissue [64].

The first analysis performed on the whole dataset of RNAseq data was an exploratory data analysis. We used at this purpose a Principal Component Analysis to reduce the complexity of the dataset and to describe the variability of gene expression data in the samples processed. From this investigation we got three major information: 1) gene expression data clearly differentiate the acute phase from the steady state, in line with the different clinical conditions observed at the two timepoints. 2) Patients at day 3 are much more heterogeneous, similarly to what the clinicians report on the patient's response to treatment that is estimated at day 3. 3) The signature

of 1748 genes identified through the comparison of gene expression across timepoints was also used to analyze the inter-patient variability of septic shock patients at day 1 (Figure 12). With the unsupervised clustering analysis we could appreciate different transcriptional responses in septic shock patients homogeneous on a clinical basis. This opens the possibility to use the transcriptome analysis to identify, also in adult septic shock, subgroups of patients with different transcriptional profile as previously reported by Wong in pediatric septic shock[62]. The inter-individual variability observed in the transcriptomic response to septic shock could be possibly related to the patient medical history, co-morbidities, genetic factors or virulence of the pathogens. At this purpose, a recent study by Davenport et al. [60] identified genetic variants influencing the expression level of key immune and metabolic genes involved in endotoxin tolerance, T cell activation, hypoxic response and switch to glycolysis.

The innate immune system is the first line of defense against infections and in collaboration with the adaptive system plays an important role in sepsis[43]. The results of our comparison between the acute phase and the steady state are in line with this, and the Gene Ontology overrepresentation analysis highlighted the role of the innate and adaptive immune response (Table 8). We observed that pathways involved in the recognition of pathogens such as Toll-like receptor and C-type lectins are transcriptionally downregulated at day 7, in accordance with their function that is mainly required in the very initial phase of sepsis when the body needs to counteract the infection [65]. Downregulation at steady state was observed also for the interleukin receptors IL1R2, IL1RAP, IL18R1, IL18RAP binding the proinflammatory cytokines IL-1 and IL-18 and for the alarmins S100A8, S100A9, S100A12, that are important mediators of inflammation[66][67][68]. These classes of molecules were described by Tsalik et al. who found higher expression in sepsis survivors vs non survivors showing that a proper activation of the inflammatory pathway in the initial response to sepsis

correlates with positive outcome [61]. Notably serum IL1R2 has been recently proposed as a new potential biomarker for the diagnosis of sepsis[69]. At day 7 we also observed the upregulation of genes involved in the adaptive immune response of T and B lymphocytes. Of note, we observed a marked upregulation of 27 immunoglobulin genes encoding the heavy chain, the light chain and the variable chain of immunoglobulins suggesting that the antibody mediated immunity is highly involved in the immunological modifications of septic shock. This is consistent with the changes in gene expression in the early phase of septic shock observed by Cazalis , who detected a downregulation of functions of the adaptive immune response (T cell signaling and antigen presentation genes) together with an increased expression of genes of acute inflammation and innate immune response[63]. Moreover several studies have reported decreased circulating immunoglobulin levels when sepsis develops, in line with the upregulation of immunoglobulin genes that we observe at T3 [70].

These observations underline that the initial phase of septic shock (day 1) is characterized by an acute inflammatory response, whereas at day 7, the pathways of Pattern recognition receptor signaling, alarmins and IL-1 proinflammatory cytokines are downregulated and the adaptive immune functions are increased in accordance to the theory described by Hotchkiss [43](Figure 2) and with the microarray study of Wong in a cohort of pediatric septic shock.[71]

Lipids and lipid mediators derived from fatty acids can influence the immune system [72][73]. In our dataset, genes encoding enzymes of the lipid pathway were differentially expressed at steady state. Among these, the free fatty acid receptor FFAR3 and the fatty acid binding protein FABP2, involved in lipid metabolism and whole body energy homeostasis[74], [75]. Genes of the prostaglandin pathway were also differentially expressed including HPGD, the major enzyme involved in the degradation of prostaglandins and the prostaglandin receptor PTGDR2 [72][76]. Prostaglandins interact with pro-

inflammatory cytokines, amplify and modulate inflammation and activate resolution [77]. Two genes of the ALOX family, ALOX15B (arachidonate 15-lipoxygenase, type B) and ALOX15 (arachidonate 15-lipoxygenase) were differentially expressed at steady state. They encode ALOX enzymes that are pivotal in the synthesis of resolvins. The expression of HPGD and ALOX genes has been described associated to clinical outcome in leukocytes of trauma patients [78]. In the same biological pathway of lipid mediators, we observed the downregulation of S1PR1, the receptor of the sphingosine-1-phosphate (SIP), a bioactive lysophospholipid generated from intracellular ceramide, a key regulator of microvascular endothelial function [79]. Microvascular endothelial dysfunction is a hallmark in sepsis in humans and is considered a predictor of outcome in patients with severe sepsis [80]. When endothelial function is impaired, the release of the vasodilator nitric oxide and prostaglandin is deregulated, vascular reactivity to vasoconstrictors is reduced, leukocytes and platelets aggregate [81].

In experimental endotoxemia Al Banna et al. [82] have reported the contribution of oxidized LDL to leukocyte activation and microvascular alterations. At steady state we found the upregulation of OLR1 also called LOX1, that is the receptor of oxidized LDL. It is thought that oxidized LDL and LOX1 may play a role in the increased inflammation and capillary leakage, two factors that induce disturbances in microcirculation. LDL levels can be regulated through the action of proprotein convertase subtilisin–kexin type 9 (PCSK9) that binds the LDL receptor (LDLR) on hepatocytes and promotes its lysosomal degradation[28]. PCSK9 was downregulated at day 7 suggesting that there is an increased LDLR activity on hepatocytes in line with the upregulation of the receptor LOX1. These observations point to a modification in the lipid homeostasis and are consistent with the alteration in fatty acid metabolism reported in sepsis by Langley in relation to the clinical outcome[49].

From it’s onset, sepsis is characterized by a hypermetabolic condition. Septic

patients have sustained fever, and they have increased need of energy supplies [83]. We found a strong downregulation at steady state of genes that encode glycolytic enzymes: hexokinase 3 (HK3) that catalyzes the phosphorylation of glucose, the first step in glycolysis and in most of glucose metabolism pathways; 6-Phosphofructo-2-Kinase (PFKFB2 and PFKFB3) that synthetize and degrade fructose-2,6-bisphosphate, a regulatory molecule that strongly activates glycolysis; IDNK a gene with gluconokinase activity. A higher expression of genes of the glycolytic pathway during the acute phase of shock could be explained by the increased anaerobic metabolism that is activated when hypoxia occurs in septic shock and causes hyperlactatemia, a common finding associated to sepsis[83], that we also observed in our cohort of patients. Hyperlactatemia is a marker of the metabolic stress response. Hyperlactatemia could also indicate an accelerated aerobic glycolysis that can occur in non-hypoxic circumstances[6]. This is an alternative explanation for sepsis-associated hyperlactatemia and the downregulation of genes of the glycolytic pathway at steady state that we observed could reflect the change in metabolic state that occurred in the acute shock condition at T1.

At day 7 we observed the increased expression of genes involved in defense mechanisms to pathogens, including the Myeloperoxidase enzyme, the serine proteases Elastase, Cathepsin G and Proteinase 3, the antimicrobial peptides Defensin Alpha 3, Defensin Alpha 4 and the Cathelicidin Antimicrobial Peptide. These molecules are expressed in neutrophil granules and partecipate in bacterial killing through several mechanisms: production of hypohalous acids (myeloperoxidase), degradation of engulfed pathogens (serine proteases) and permeabilization of bacterial plasma membrane (antimicrobial peptides) [84]. We hypothesize that the increased expression of antimicrobial systems in the steady state of shock could be useful to control the primary infection and prevent secondary infections, which in a recent study were estimate to affect 13% of sepsis patients [85]. The

Cathelicidin Antimicrobial Peptide has been also associated to suppression of the pyroptosis of macrophages and inflammatory cytokine production in a murine model of sepsis [86] suggesting that it could be implicated in the decrease of the inflammatory state observed in the first week after the ICU admission. Beyond Neutrophil serine proteases, we observed the modulation of several genes with protease activity. In our patients at T3 the metalloproteases MMP8 and MMP9, decrease their level of expression. Accordingly, in the FINNSEPSIS study cohort both MMP8 and MMP9 were upregulated in early phase of severe sepsis compared to healthy controls and high serum level of MMP8 have been associated to fatal outcome [87]. Metalloproteases can degrade extracellular matrix proteins, modulate the inflammatory responses and tissue repair [88] and can modify blood pressure by several mechanisms [89]. ADAMTS3 metallopeptidase involved in the cleavage of propeptides of type II collagen, showed the same downregulated expression trend suggesting that ADAMTS3 could participate in the extracellular matrix remodeling in septic shock. Upregulation was observed for MME, the metalloendopeptidase neprilysin involved in the inactivation of several peptide hormons like angiotensins and the atrial natriuretic factor, and previously associated to outcome in acute heart failure[90]. PLAU, the plasminogen activator urokinase involved in fibrin degradation, coagulation[91], cardiac fibrosis[92] and heart failure [93] was upregulated as well. These findings indicates a potential role of proteases in the regulation of factors affecting the cardiovascular system in septic shock and are in line with the work of Sharony et al.[94], which highlights the role of proteases in the cardiovascular system. These results support the hypothesis that proteases could be an important factor in the development of circulatory shock and subsequent multiorgan failure as suggested by previous studies on the role of intestinal proteases in shock [95].

At steady state, we observed an increased expression of genes involved in protein synthesis such as structural constituent of ribosomes and genes

involved in control of translation. A reduction of protein synthesis has been previously observed by Vary and Kimball[96] in muscles of septic rats. Our transcriptomic data suggest that a similar reduction in protein synthesis occurs also in human blood cells, in the acute phase of septic shock. This could be a conservative metabolic strategy, promoting cell survival by inhibiting biological processes not essential during the critical condition of day 1. A decreased expression of genes involved in the transport of vesicles from the endoplasmic reticulum to Golgi was observed at day 7, particularly regarding vesicles coated with COPII proteins. This observation, together with the high number of identified DEGs related to extracellular exosomes, suggest there could be an increased release of vesicles in the extracellular space in the acute phase of septic shock. This is consistent with a recent finding by Lehner et al.[97] who detected a higher number of circulating microvesicles released by platelets and leukocytes in septic shock patients compared to controls.

Previous transcriptomic analysis in sepsis and septic shock were mainly focused on expression of coding genes or microRNAs [60], [61], [63], [98]. Our analysis explored not only coding RNAs and microRNAs, but also long noncoding RNAs. Long noncoding RNAs (lncRNAs) have gained attention as potential new biological regulators and have been implicated in a range of developmental processes and diseases [99]. Long ncRNAs can play a fine regulatory role of gene expression through mechanisms of mediated RNA decay or acting as decoys for miRNAs[100]. Our analysis identified 30 lncRNAs differentially expressed in septic shock comparing T1 to T3. Among these, LINC01127 was downregulated at T3 in the RNASeq analysis. The function of LINC01127 is unknown, but its genomic position, upstream the genes coding the receptors of IL-1 and IL-18, suggests that it could play a role in the context of acute inflammation. The long ncRNA MIAT, downregulated at steady state, is reported as a transcript associated to

myocardial infarction and plays a role in cardiac hypertrophy by sponging mir-150[101].

Comparing day 1 to day 7, we observed the differential expression of some microRNAs. miR-125a-5p and miR-150-5p, that are upregulated at day 7, were previously reported as markers of sepsis, when septic patients were compared with healthy controls[98]. In line with the case control study of septic patients vs healthy subjects of Ma et al., we observed a low level of miR-125a-5p and miR-150-5p during the acute phase of septic shock and a higher level at steady state, suggesting that their regulatory activity is reduced during the acute phase of shock and then recovered at steady state. The “in silico” search for their target genes indicated that miR-125a-5p and miR-150-5p could have a role in the regulation of the MAPK pathway. In detail, their upregulation at day 7 could result in an inhibitory action of the MAPK pathway. On the contrary, in the acute phase, downregulation of miR-125a-5p and miR150-5p could result in the activation of the MAPK pathway that is involved in the signaling cascade of toll-like receptor[102] and of the inflammatory pathways[103], that are important pathways in septic shock. miR-150 was previously linked to cardiac hypertrophy and fibrosis and its availability is under the control of the long ncRNA MIAT, which was also identified in our analysis [101]. We speculate that these two molecules could be involved in the cardiovascular complications of sepsis that can lead the patient to acute heart failure. Downregulation at steady state was also observed for miR-193a-3p. Among its predicted targets PLAU, the plasminogen activator urokinase, is an important factor controlling blood coagulation with a beneficial effect against disseminated intravascular coagulation that is often associated to septic shock[104].

6 CONCLUSION

In this work our aim was to illustrate the complex modifications of blood cell transcriptomic profile in septic shock in a well characterized cohort at three timepoints. We identified two major transcriptomic profiles, corresponding to the clinical conditions of acute phase (day 1) and steady state of shock (day 7) and we showed that different groups of patients can be identified based on their –omic profile. The expression profile of the two conditions was different in multiple pathways, including the pathways of innate and adaptive immune response, metabolic pathways of lipids and glycolysis, antimicrobial systems, proteases and processes involving extracellular vesicles. These findings supported the results of previous works in sepsis and septic shock with the added value to analyze the patients during a period of 7 days. We proposed that miR-125a-5p and miR-150-5p could have a regulatory role on the MAPK pathway in septic shock and we newly identified 30 long ncRNAs differentially expressed between the acute phase and steady state. Future investigations will concern the analysis in the same cohort of the expression profile in relation to the clinical outcomes and the response to therapy.

7 BIBLIOGRAPHY

[1] M. Singer, C. S. Deutschman, C. W. Seymour, M. Shankar-Hari, D. Annane, M. Bauer, R. Bellomo, G. R. Bernard, J.-D. Chiche, C. M. Coopersmith, R. S. Hotchkiss, M. M. Levy, J. C. Marshall, G. S. Martin, S. M. Opal, G. D. Rubenfeld, T. van der Poll, J. Vincent, and D. C. Angus, "The Third International Consensus Definitions for Sepsis and Septic Shock (Sepsis-3).," *Jama*, vol. 315, no. 8, pp. 801–10, 2016.

[2] G. S. Martin, D. M. Mannino, and M. Moss, "The effect of age on the development and outcome of adult sepsis.," *Crit. Care Med.*, vol. 34, no. 1, pp. 15–21, 2006.

[3] G. S. Martin, D. M. Mannino, S. Eaton, and M. Moss, "The epidemiology of sepsis in the United States from 1979 through 2000.," *N. Engl. J. Med.*, vol. 348, no. 16, pp. 1546–54, 2003.

[4] A. M. Esper, M. Moss, C. A. Lewis, R. Nisbet, D. M. Mannino, and G. S. Martin, "The role of infection and comorbidity: Factors that influence disparities in sepsis.," *Crit. Care Med.*, vol. 34, no. 10, pp. 2576–82, 2006.

[5] P. A. Ward, "New approaches to the study of sepsis," *EMBO Mol. Med.*, vol. 4, no. 12, pp. 1234–1243, 2012.

[6] M. Garcia-alvarez, P. Marik, and R. Bellomo, "Sepsis-associated hyperlactatemia," pp. 1–11, 2014.

[7] J. Cohen, J. L. Vincent, N. K. J. Adhikari, F. R. Machado, D. C. Angus, T. Calandra, K. Jaton, S. Giulieri, J. Delaloye, S. Opal, K. Tracey, T. van der Poll, and E. Pelfrene, "Sepsis: A roadmap for future research," *Lancet Infect. Dis.*, vol. 15, no. 5, pp. 581–614, 2015.

[8] D. C. Angus, W. T. Linde-Zwirble, J. Lidicker, G. Clermont, J. Carcillo, and M. R. Pinsky, "Epidemiology of severe sepsis in the United States: analysis of incidence, outcome, and associated costs of care.," *Crit.*

Care Med., vol. 29, no. 7, pp. 1303–1310, 2001.

[9] G. Pawelec, R. Solana, E. Remarque, and E. Mariani, “Impact of aging on innate immunity.,” *J Leukoc Biol*, vol. 64, no. 6, pp. 703–712, 1998.

[10] H. Bruunsgaard, P. Skinhoj, J. Qvist, and B. K. Pedersen, “Elderly humans show prolonged in vivio inflammatory activity during pneumococcal infections,” *J. Infect. Dis.*, vol. 180, pp. 551–554, 1999.

[11] J.-L. Vincent, Y. Sakr, C. L. Sprung, V. M. Ranieri, K. Reinhart, H. Gerlach, R. Moreno, J. Carlet, J.-R. Le Gall, and D. Payen, “Sepsis in European intensive care units: results of the SOAP study.,” *Crit. Care Med.*, vol. 34, no. 2, pp. 344–353, 2006.

[12] T. J. Iwashyna, E. W. Ely, D. M. Smith, and K. M. Langa, “Long-term Cognitive Impairment and Functional Disability Among Survivors of Severe Sepsis,” vol. 304, no. 16, pp. 1787–1794, 2016.

[13] R. S. Hotchkiss, L. L. Moldawer, S. M. Opal, K. Reinhart, I. R. Turnbull, and J.-L. Vincent, “Sepsis and septic shock,” *Nat. Rev. Dis. Prim.*, vol. 2, no. August, p. 16045, 2016.

[14] A. Kumar, P. Ellis, and Y. Arabi, “Initiation of Inappropriate Antimicrobial Therapy Results in a Fivefold Reduction of Survival in Human Septic Shock,” *Chest*, vol. 136, no. 5, pp. 1237–1248, 2009.

[15] J.-L. Vincent, A. de Mendonca, F. Cantraine, R. Moreno, J. Takala, P. M. Suter, C. L. Sprung, F. Colardyn, and S. Blecher, “Use of the SOFA score to assess the incidence of organ dysfunction/failure in intensive care units,” *Crit. Care Med.*, vol. 26, no. 11, pp. 1793–1800, 1998.

[16] K. J. Ishii, S. Koyama, A. Nakagawa, C. Coban, and S. Akira, “Host Innate Immune Receptors and Beyond: Making Sense of Microbial Infections,” *Cell Host Microbe*, vol. 3, no. 6, pp. 352–363, 2008.

[17] P. Matzinger, “The danger model: a renewed sense of self,” *Science (80-.).*, vol. 296, pp. 301–305, 2002.

[18] E. Meylan, J. Tschopp, and M. Karin, “Intracellular pattern recognition receptors in the host response,” *Nature*, vol. 442, no. July, pp. 39–44,

2006.

[19] T. B. H. Geijtenbeek and S. I. Gringhuis, “Signalling through C-type lectin receptors: shaping immune responses.,” *Nat. Rev. Immunol.*, vol. 9, no. 7, pp. 465–79, 2009.

[20] N. M. Foley, J. Wang, H. Redmond, and J. Wang, “Current knowledge and future directions of TLR and NOD signaling in sepsis,” *Mil. Med. Res.*, vol. 2, no. 1, p. 1, 2015.

[21] S. K. Biswas and E. Lopez-Collazo, “Endotoxin tolerance: new mechanisms, molecules and clinical significance,” *Trends in Immunology*, vol. 30, no. 10. pp. 475–487, 2009.

[22] M. Lamkanfi Sarkar, A., Vande Walle, L., Vitari, A. C., Amer, A. O., Wewers, M D., Tracey, K. J., Kanneganti, T.-D., Dixit, V. M., “Inflammasome-dependent release of the alarmin HMGB1 in endotoxemia,” *J. Immunol.*, vol. 185, no. 7, pp. 4385–4392, 2010.

[23] P. A. Ward and H. Gao, “Sepsis, complement and the dysregulated inflammatory response,” *J. Cell. Mol. Med.*, vol. 13, no. 10, pp. 4154–4160, 2009.

[24] J. E. Gotts and M. A. Matthay, “Sepsis: pathophysiology and clinical management,” *Bmj*, vol. 353, p. i1585, 2016.

[25] D. C. (Pitt) Angus and T. van der Poll, “Severe sepsis and septic shock.,” *N. Engl. J. Med.*, vol. 369, no. 9, pp. 840–51, 2013.

[26] Y. Kakihana, T. Ito, M. Nakahara, K. Yamaguchi, and T. Yasuda, “Sepsis-induced myocardial dysfunction; pathophysiology and management,” *J. Intensive Care*, vol. 4, p. 22, 2016.

[27] G. W. Schmid-Schönbein and M. Chang, “The autodigestion hypothesis for shock and multi-organ failure,” in *Annals of Biomedical Engineering*, 2014, vol. 42, no. 2, pp. 405–414.

[28] K. R. Walley, G. A. Francis, S. M. Opal, E. A. Stein, J. A. Russell, and J. H. Boyd, “The central role of proprotein convertase subtilisin/kexin type 9 in septic pathogen lipid transport and clearance,” *Am. J. Respir.*

Crit. Care Med., vol. 192, no. 11, pp. 1275–1286, 2015.

[29] J. R. Prowle and R. Bellomo, “Sepsis-Associated Acute Kidney Injury: Macrohemodynamic and Microhemodynamic Alterations in the Renal Circulation,” *Semin. Nephrol.*, vol. 35, no. 1, pp. 64–74, 2015.

[30] R. Alobaidi, R. K. Basu, S. L. Goldstein, and S. M. Bagshaw, “Sepsis-Associated Acute Kidney Injury,” *Seminars in Nephrology*, vol. 35, no. 1. pp. 2–11, 2015.

[31] M. Ziaja, “Septic encephalopathy topical collection on infection,” *Curr. Neurol. Neurosci. Rep.*, vol. 13, no. 10, 2013.

[32] P. Schramm, K. U. Klein, L. Falkenberg, M. Berres, D. Closhen, K. J. Werhahn, M. David, C. Werner, and K. Engelhard, “Impaired cerebrovascular autoregulation in patients with severe sepsis and sepsis-associated delirium.,” *Crit. Care*, vol. 16, no. 5, p. R181, 2012.

[33] A. M. Drewry, N. Samra, L. P. Skrupky, B. M. Fuller, S. M. Compton, and R. S. Hotchkiss, “Persistent lymphopenia after diagnosis of sepsis predicts mortality.,” *Shock*, vol. 42, no. 5, pp. 383–91, 2014.

[34] R. Taneja, A. P. Sharma, M. B. Hallett, G. P. Findlay, and M. R. Morris, “Immature Circulating Neutrophils in Sepsis Have Impaired Phagocytosis and Calcium Signaling,” *Shock*, vol. 30, no. 6, pp. 618–622, 2008.

[35] J. S. Boomer, K. To, K. C. Chang, O. Takasu, D. F. Osborne, A. H. Walton, T. L. Bricker, S. D. Jarman, D. Kreisel, A. S. Krupnick, A. Srivastava, P. E. Swanson, J. M. Green, and R. S. Hotchkiss, “Immunosuppression in patients who die of sepsis and multiple organ failure.,” *JAMA*, vol. 306, no. 23, pp. 2594–605, 2011.

[36] M. Hynninen, V. Pettilä, O. Takkunen, R. Orko, S.-E. Jansson, P. Kuusela, R. Renkonen, and M. Valtonen, “Predictive value of monocyte histocompatibility leukocyte antigen-DR expression and plasma interleukin-4 and -10 levels in critically ill patients with sepsis.,” *Shock*, vol. 20, no. 1, pp. 1–4, 2003.

[37] R. S. Hotchkiss, K. W. Tinsley, P. E. Swanson, K. C. Chang, J. P. Cobb, T. G. Buchman, S. J. Korsmeyer, and I. E. Karl, “Prevention of lymphocyte cell death in sepsis improves survival in mice.,” *Proc. Natl. Acad. Sci. U. S. A.*, vol. 96, no. 25, pp. 14541–6, 1999.

[38] R. S. Hotchkiss, R. E. Schmieg, P. E. Swanson, B. D. Freeman, K. W. Tinsley, J. P. Cobb, I. E. Karl, T. G. Buchman, and R. E. S. Jr, “Rapid onset of intestinal epithelial and lymphocyte apoptotic cell death in patients with trauma and shock.,” *Crit. Care Med.*, vol. 28, no. 9, pp. 3207–17, 2000.

[39] R. E. Voll, M. Herrmann, E. A. Roth, C. Stach, J. R. Kalden, and I. Girkontaite, “Immunosuppressive effects of apoptotic cells.,” *Nature*, vol. 390, no. 6658, pp. 350–1, 1997.

[40] D. R. Green and H. M. Beere, “Apoptosis. Gone but not forgotten.,” *Nature*, vol. 405, no. 6782, pp. 28–29, 2000.

[41] G. P. Otto, M. Sossdorf, R. A. Claus, J. Rödel, K. Menge, K. Reinhart, M. Bauer, and N. C. Riedemann, “The late phase of sepsis is characterized by an increased microbiological burden and death rate.,” *Crit. Care*, vol. 15, no. 4, p. R183, 2011.

[42] A. H. Walton, J. T. Muenzer, D. Rasche, J. S. Boomer, B. Sato, B. H. Brownstein, A. Pachot, T. L. Brooks, E. Deych, W. D. Shannon, J. M. Green, G. A. Storch, and R. S. Hotchkiss, “Reactivation of multiple viruses in patients with sepsis,” *PLoS One*, vol. 9, no. 2, p. e98819, 2014.

[43] R. S. Hotchkiss, G. Monneret, and D. Payen, “Sepsis-induced immunosuppression: from cellular dysfunctions to immunotherapy.,” *Nat. Rev. Immunol.*, vol. 13, no. 12, pp. 862–874, 2013.

[44] D. Brealey, M. Brand, I. Hargreaves, S. Heales, J. Land, R. Smolenski, N. A. Davies, C. E. Cooper, and M. Singer, “Association between mitochondrial dysfunction and severity and outcome of septic shock,” *Lancet*, vol. 360, no. 9328, pp. 219–223, 2002.

[45] C. S. Deutschman and K. J. Tracey, “Sepsis: Current dogma and new perspectives,” *Immunity*, vol. 40, no. 4, pp. 463–475, 2014.

[46] Z. a Puthucheary, J. Rawal, M. McPhail, B. Connolly, G. Ratnayake, P. Chan, N. S. Hopkinson, R. Phadke, R. Padhke, T. Dew, P. S. Sidhu, C. Velloso, J. Seymour, C. C. Agley, A. Selby, M. Limb, L. M. Edwards, K. Smith, A. Rowlerson, M. J. Rennie, J. Moxham, S. D. R. Harridge, N. Hart, and H. E. Montgomery, “Acute skeletal muscle wasting in critical illness.,” *JAMA*, vol. 310, no. 15, pp. 1591–600, 2013.

[47] W. H. Hartl and K. W. Jauch, “Metabolic self-destruction in critically ill patients: Origins, mechanisms and therapeutic principles,” *Nutrition*, vol. 30, no. 3, pp. 261–267, 2014.

[48] M. Ferrario, A. Cambiaghi, L. Brunelli, S. Giordano, P. Caironi, L. Guatteri, F. Raimondi, L. Gattinoni, R. Latini, S. Masson, G. Ristagno, and R. Pastorelli, “Mortality prediction in patients with severe septic shock : a pilot study using a target metabolomics approach,” *Nat. Publ. Gr.*, no. August 2015, pp. 1–11, 2016.

[49] R. J. Langley, E. L. Tsalik, J. C. van Velkinburgh, S. W. Glickman, B. J. Rice, C. Wang, B. Chen, L. Carin, A. Suarez, R. P. Mohney, D. H. Freeman, M. Wang, J. You, J. Wulff, J. W. Thompson, M. A. Moseley, S. Reisinger, B. T. Edmonds, B. Grinnell, D. R. Nelson, D. L. Dinwiddie, N. a Miller, C. J. Saunders, S. S. Soden, A. J. Rogers, L. Gazourian, L. E. Fredenburgh, A. F. Massaro, R. M. Baron, A. M. K. Choi, G. R. Corey, G. S. Ginsburg, C. B. Cairns, R. M. Otero, V. G. Fowler, E. P. Rivers, C. W. Woods, and S. F. Kingsmore, “An integrated clinico-metabolomic model improves prediction of death in sepsis.,” *Sci. Transl. Med.*, vol. 5, no. 195, p. 195ra95, Jul. 2013.

[50] D. W. Park, D. S. Kwak, Y. Y. Park, Y. Chang, J. W. Huh, C. M. Lim, Y. Koh, D. K. Song, and S. B. Hong, “Impact of serial measurements of lysophosphatidylcholine on 28-day mortality prediction in patients admitted to the intensive care unit with severe sepsis or septic shock,”

J. Crit. Care, vol. 29, no. 5, p. 882.e5-882.e11, 2014.

[51] K. Reinhart, M. Bauer, N. C. Riedemann, and C. S. Hartog, “New approaches to sepsis: Molecular diagnostics and biomarkers,” *Clin. Microbiol. Rev.*, vol. 25, no. 4, pp. 609–634, 2012.

[52] D. S. DeLuca, J. Z. Levin, A. Sivachenko, T. Fennell, M.-D. Nazaire, C. Williams, M. Reich, W. Winckler, and G. Getz, “RNA-SeQC: RNA-seq metrics for quality control and process optimization.,” *Bioinformatics*, vol. 28, no. 11, pp. 1530–2, Jun. 2012.

[53] Y. Liao, G. K. Smyth, and W. Shi, “FeatureCounts: An efficient general purpose program for assigning sequence reads to genomic features,” *Bioinformatics*, vol. 30, no. 7, pp. 923–930, 2014.

[54] M. I. Love, W. Huber, and S. Anders, “Moderated estimation of fold change and dispersion for RNA-seq data with DESeq2.,” *Genome Biol.*, vol. 15, no. 12, p. 550, 2014.

[55] D. W. Huang, R. a Lempicki, and B. T. Sherman, “Systematic and integrative analysis of large gene lists using DAVID bioinformatics resources.,” *Nat. Protoc.*, vol. 4, no. 1, pp. 44–57, 2009.

[56] B. P. Lewis, C. B. Burge, and D. P. Bartel, “Conserved seed pairing, often flanked by adenosines, indicates that thousands of human genes are microRNA targets,” *Cell*, vol. 120, no. 1, pp. 15–20, 2005.

[57] V. Agarwal, G. W. Bell, J. W. Nam, and D. P. Bartel, “Predicting effective microRNA target sites in mammalian mRNAs,” *Elife*, vol. 4, no. AUGUST2015, 2015.

[58] R. C. Friedman, K. K. H. Farh, C. B. Burge, and D. P. Bartel, “Most mammalian mRNAs are conserved targets of microRNAs,” *Genome Res.*, vol. 19, no. 1, pp. 92–105, 2009.

[59] F. Aletti, C. Conti, M. Ferrario, V. Ribas, B. B. Pinto, A. Herpain, E. Post, E. R. Medina, C. Barlassina, E. De Oliveira, R. Pastorelli, G. Tedeschi, G. Ristagno, F. S. Taccone, G. W. Schmid-schönbein, R. Ferrer, D. De Backer, K. Bendjelid, and G. Baselli, “ShockOmics :

multiscale approach to the identification of molecular biomarkers in acute heart failure induced by shock," *Scand. J. Trauma. Resusc. Emerg. Med.*, vol. 24, no. 9, 2016.

[60] E. E. Davenport, K. L. Burnham, J. Radhakrishnan, P. Humburg, P. Hutton, T. C. Mills, A. Rautanen, A. C. Gordon, C. Garrard, A. V. S. Hill, C. J. Hinds, and J. C. Knight, "Genomic landscape of the individual host response and outcomes in sepsis: A prospective cohort study," *Lancet Respir. Med.*, vol. 4, no. 4, pp. 259–271, 2016.

[61] E. L. Tsalik, R. J. Langley, D. L. Dinwiddie, N. A. Miller, B. Yoo, J. C. van Velkinburgh, L. D. Smith, I. Thiffault, A. K. Jaehne, A. M. Valente, R. Henao, X. Yuan, S. W. Glickman, B. J. Rice, M. T. McClain, L. Carin, G. R. Corey, G. S. Ginsburg, C. B. Cairns, R. M. Otero, V. G. Fowler, E. P. Rivers, C. W. Woods, and S. F. Kingsmore, "An integrated transcriptome and expressed variant analysis of sepsis survival and death," *Genome Med.*, vol. 6, no. 11, p. 111, 2014.

[62] H. R. Wong, N. Cvijanovich, R. Lin, G. L. Allen, N. J. Thomas, D. F. Willson, R. J. Freishtat, N. Anas, K. Meyer, P. a Checchia, M. Monaco, K. Odom, and T. P. Shanley, "Identification of pediatric septic shock subclasses based on genome-wide expression profiling.," *BMC Med.*, vol. 7, p. 34, Jan. 2009.

[63] M.-A. Cazalis, A. Lepape, F. Venet, F. Frager, B. Mougin, H. Vallin, M. Paye, A. Pachot, and G. Monneret, "Early and dynamic changes in gene expression in septic shock patients : a genome-wide approach," *Intensive Care Med. Exp.*, vol. 2, no. 20, 2014.

[64] C. C. Liew, J. Ma, H. C. Tang, R. Zheng, and A. A. Dempsey, "The peripheral blood transcriptome dynamically reflects system wide biology: A potential diagnostic tool," *J. Lab. Clin. Med.*, vol. 147, no. 3, pp. 126–132, 2006.

[65] H. Tsujimoto, S. Ono, P. A. Efron, P. O. Scumpia, L. L. Moldawer, and H. Mochizuki, "Role of Toll-like receptors in the development of

sepsis.," *Shock*, vol. 29, no. 3, pp. 315–21, 2008.

[66] J.-C. Simard, A. Cesaro, J. Chapeton-Montes, M. Tardif, F. Antoine, D. Girard, and P. a Tessier, "S100A8 and S100A9 induce cytokine expression and regulate the NLRP3 inflammasome via ROS-dependent activation of NF-κB(1.)," *PLoS One*, vol. 8, no. 8, p. e72138, 2013.

[67] C. A. Dinarello, "Interleukin-1 in the pathogenesis and treatment of inflammatory diseases," *Blood*, vol. 117, no. 14, pp. 3720–3732, 2011.

[68] C. A. Dinarello, "Interleukin 1 and interleukin 18 as mediators of inflammation and the aging process," *Am. J. Clin. Nutr.*, vol. 83, no. 2, 2006.

[69] Y. Lang, Y. Jiang, M. Gao, W. Wang, N. Wang, K. Wang, H. Zhang, G. Chen, K. Liu, M. Liu, M. Yang, and X. Xiao, "Interleukin-1 Receptor 2: A New Biomarker for Sepsis Diagnosis and GramNegative/ GramPositive Bacterial Differentiation.," *Shock*, vol. 47, no. 1, pp. 119–124, 2017.

[70] E. J. Giamarellos-Bourboulis and S. M. Opal, "The role of genetics and antibodies in sepsis.," *Ann. Transl. Med.*, vol. 4, no. 17, p. 328, 2016.

[71] H. R. Wong, "Genome-wide expression profiling in pediatric septic shock," *Pediatr Res*, vol. 73, no. 4, pp. 564–569, 2013.

[72] B. Samuelsson, "Role of basic science in the development of new medicines: examples from the eicosanoid field," *J. Biol. Chem.*, vol. 287, no. 13, pp. 10070–10080, 2012.

[73] A. J. de Jong, M. Kloppenburg, R. E. M. Toes, and A. Ioan-Facsinay, "Fatty acids, lipid mediators, and T-cell function," *Frontiers in Immunology*, vol. 5, no. OCT. 2014.

[74] A. M. Gajda and J. Storch, "Enterocyte fatty acid-binding proteins (FABPs): Different functions of liver and intestinal FABPs in the intestine," *Prostaglandins Leukot. Essent. Fat. Acids*, vol. 93, pp. 9–16, 2015.

[75] T. Hara, I. Kimura, D. Inoue, A. Ichimura, and A. Hirasawa, “Free fatty acid receptors and their role in regulation of energy metabolism,” *Rev. Physiol. Biochem. Pharmacol.*, vol. 159, pp. 1–77, 2013.

[76] C. M. Ensor and H. H. Tai, “15-Hydroxyprostaglandin dehydrogenase,” *J. Lipid Mediat. Cell Signal.*, vol. 12, no. 2–3, pp. 313–319, 1995.

[77] C. N. Serhan, “Pro-resolving lipid mediators are leads for resolution physiology.,” *Nature*, vol. 510, no. 7503, pp. 92–101, 2014.

[78] S. K. Orr, K. L. Butler, D. Hayden, R. G. Tompkins, C. N. Serhan, and D. Irimia, “Gene Expression of Proresolving Lipid Mediator Pathways Is Associated With Clinical Outcomes in Trauma Patients,” *Crit Care Med*, vol. 43, no. 12, pp. 2642–2650, 2015.

[79] Y. Zeng, R. H. Adamson, F.-R. E. Curry, and J. M. Tarbell, “Sphingosine-1-phosphate protects endothelial glycocalyx by inhibiting syndecan-1 shedding.,” *Am. J. Physiol. Heart Circ. Physiol.*, vol. 306, no. 3, pp. H363-72, 2014.

[80] D. De Backer, K. Donadello, Y. Sakr, G. Ospina-Tascon, D. Salgado, S. Scolletta, and J. L. Vincent, “Microcirculatory alterations in patients with severe sepsis: impact of time of assessment and relationship with outcome,” *Crit Care Med*, vol. 41, no. 3, pp. 791–799, 2013.

[81] J. Boisramé-Helms, H. Kremer, V. Schini-Kerth, and F. Meziani, “Endothelial dysfunction in sepsis.,” *Curr. Vasc. Pharmacol.*, vol. 11, no. 2, pp. 150–60, 2013.

[82] N. Al-Banna and C. Lehmann, “Oxidized LDL and LOX-1 in experimental sepsis,” *Mediators of Inflammation*, vol. 2013. 2013.

[83] J. Pravda, “Metabolic theory of septic shock.,” *World J. Crit. care Med.*, vol. 3, no. 2, pp. 45–54, 2014.

[84] C. T. N. Pham, “Neutrophil serine proteases: specific regulators of inflammation.,” *Nat. Rev. Immunol.*, vol. 6, no. 7, pp. 541–50, 2006.

[85] L. A. van Vught, P. M. C. Klein Klouwenberg, C. Spitoni, B. P.

Scicluna, M. A. Wiewel, J. Horn, M. J. Schultz, P. Nürnberg, M. J. M. Bonten, O. L. Cremer, and T. van der Poll, “Incidence, Risk Factors, and Attributable Mortality of Secondary Infections in the Intensive Care Unit After Admission for Sepsis,” *Jama*, vol. 315, no. 14, p. 1469, 2016.

[86] Z. Hu, T. Murakami, K. Suzuki, H. Tamura, J. Reich, K. Kuwahara-Arai, T. Iba, and I. Nagaoka, “Antimicrobial cathelicidin peptide LL-37 inhibits the pyroptosis of macrophages and improves the survival of polybacterial septic mice,” *Int. Immunol.*, vol. 28, no. 5, pp. 245–253, 2016.

[87] A. Lauhio, J. Hästbacka, V. Pettilä, T. Tervahartiala, S. Karlsson, T. Varpula, M. Varpula, E. Ruokonen, T. Sorsa, and E. Kolho, “Serum MMP-8, -9 and TIMP-1 in sepsis: High serum levels of MMP-8 and TIMP-1 are associated with fatal outcome in a multicentre, prospective cohort study. Hypothetical impact of tetracyclines,” *Pharmacol. Res.*, vol. 64, no. 6, pp. 590–594, 2011.

[88] W. C. Parks, C. L. Wilson, and Y. S. Lopez-Boado, “Matrix metalloproteinases as modulators of inflammation and Innate Immunity,” *Nat. Rev. Immunol.*, vol. 4, no. 8, pp. 617–29, 2004.

[89] J. J. Cena, M. M. Lalu, W. J. Cho, A. K. Chow, M. L. Bagdan, E. E. Daniel, M. M. Castro, and R. Schulz, “Inhibition of matrix metalloproteinase activity in vivo protects against vascular hyporeactivity in endotoxemia.,” *Am. J. Physiol. Heart Circ. Physiol.*, vol. 298, no. 1, pp. H45–H51, 2010.

[90] A. Bayés-Genís, J. Barallat, D. Pascual, J. Nuñez, G. Miñana, J. Sánchez-Mas, A. Galan, J. Sanchis, E. Zamora, M. T. Pérez-Martínez, and J. Lupón, “Prognostic Value and Kinetics of Soluble Neprilysin in Acute Heart Failure. A Pilot Study.,” *JACC Hear. Fail.*, vol. 3, no. 8, pp. 641–644, 2015.

[91] G. Cesarman-Maus and K. A. Hajjar, “Molecular mechanisms of

fibrinolysis," *Br. J. Haematol.*, vol. 129, no. 3, pp. 307–321, 2005.

[92] A. Stempien-Otero, A. Plawman, J. Meznarich, T. Dyamenahalli, G. Otsuka, and D. A. Dichek, "Mechanisms of cardiac fibrosis induced by urokinase plasminogen activator," *J. Biol. Chem.*, vol. 281, no. 22, pp. 15345–15351, 2006.

[93] Y. Borne, M. Persson, O. Melander, J. G. Smith, and G. Engstrom, "Increased plasma level of soluble urokinase plasminogen activator receptor is associated with incidence of heart failure but not atrial fibrillation," *Eur J Hear. Fail*, vol. 16, no. 4, pp. 377–383, 2014.

[94] R. Sharony, P.-J. Yu, J. Park, A. C. Galloway, P. Mignatti, and G. Pintucci, "Protein targets of inflammatory serine proteases and cardiovascular disease.," *J. Inflamm.*, vol. 7, no. 1, p. 45, 2010.

[95] G. W. Schmid-Shönbein, "Inflammation and the Autodigestive Hypothesis," *Microcirculation*, vol. 16, no. 4, pp. 289–306, 2010.

[96] T. C. Vary and S. R. Kimball, "Sepsis-Induced Changes in Protein Synthesis: Differential Effects on Fast- and Slow-Twitch Muscles," *Am. J. Physiol.*, vol. 262, no. 6, pp. C1513–C1519, 1992.

[97] G. F. Lehner, U. Harler, V. M. Haller, C. Feistritzer, J. Hasslacher, S. Dunzendorfer, R. Bellmann, and M. Joannidis, "Characterization of Microvesicles in Septic Shock Using High-Sensitivity Flow Cytometry.," *Shock*, vol. 46, no. 4, pp. 373–381, 2016.

[98] Y. Ma, D. Vilanova, K. Atalar, O. Delfour, J. Edgeworth, M. Ostermann, M. Hernandez-Fuentes, S. Razafimahatratra, B. Michot, D. H. Persing, I. Ziegler, B. Törös, P. Mölling, P. Olcén, R. Beale, and G. M. Lord, "Genome-Wide Sequencing of Cellular microRNAs Identifies a Combinatorial Expression Signature Diagnostic of Sepsis," *PLoS One*, vol. 8, no. 10, 2013.

[99] J. T. Y. Kung, D. Colognori, and J. T. Lee, "Long noncoding RNAs: Past, present, and future," *Genetics*, vol. 193, no. 3. pp. 651–669, 2013.

[100] K. C. Wang and H. Y. Chang, “Molecular Mechanisms of Long Noncoding RNAs,” *Molecular Cell*, vol. 43, no. 6. pp. 904–914, 2011.

[101] X. Zhu, Y. Yuan, and S. Rao, “LncRNA MIAT enhances cardiac hypertrophy partly through sponging miR-150,” *Eur. Rev. Med. Pharmacol. Sci.*, vol. 20, pp. 3653–3660, 2016.

[102] S. Akira and K. Takeda, “Toll-like receptor signalling.,” *Nat. Rev. Immunol.*, vol. 4, no. 7, pp. 499–511, 2004.

[103] T. Zarubin and J. Han, “Activation and signaling of the p38 MAP kinase pathway.,” *Cell Res.*, vol. 15, no. 1, pp. 11–18, 2005.

[104] Y. Vasquez, C. H. Williams, and R. M. Hardaway, “Effect of urokinase on disseminated intravascular coagulation,” *J. Appl. Physiol.*, vol. 85, no. 4, pp. 1421–1428, 1998.

8 APPENDIX

Gene Ontology	Genes
GO:0038096:Fc-gamma receptor signaling pathway involved in phagocytosis	IGHG1, IGHG2, IGHG3, IGHG4, FGR, IGHV3-48, IGKV1-17, CD247, ARPC4, ABI1, ARPC5, ACTR3, ACTR2, CDC42, ARPC3, ARPC2, FCGR1A, IGHV3-23, PIK3CA, IGKC, SYK, IGLV1-51, CD3G, HCK, NCKAP1L, ELMO2, ARPC1A, IGHV3-30, ARPC1B, IGKV1-5, MYO10, IGHV3-7, IGHV4-39, IGHV3-33,
GO:0038095:Fc-epsilon receptor signaling pathway	IGHV3-48, IGKV1-17, NFKBIA, NFKB1, BTK, PSMB6, PSMB3, MAP3K1, IGHV3-23, PSMD1, PIK3CA, FCER1G, PSMD5, IGKC, NFATC2, PSMD6, FBXW11, PSMD7, CHUK, RPS27A, SYK, FCER1A, ITK, IGLV1-51, IGHV3-30, NRAS, CARD11, IGKV1-5, PSMC6, IGHV3-7, LAT2, IGHV4-39, IGHV3-33, PSMA6, PLCG1, PSMD12, PSMD10, PSMC1, IGLV7-43, IGKV4-1, IGKV3-20, IGLC2, IGLC3
GO:0045087:innate immune response	IGHG1, IGHG2, IGHG3, IGHG4, S100A8, TBK1, CAPZA2, CAPZA1, PPARG, S100A9, TLR1, TLR2, TLR4, NFKB1, TLR5, IGHM, FES, TLR7, LGR4, TLR8, BTK, MARCO, NLRC4, MAP3K5, SH2D1A, NOD2, CLEC4E, CD46, LILRA5, IL1RAP, VNN1, CLEC4D, RPS27A, CHUK, SYK, MATK, F12, LY96, CAMP, GZMM, C1QB, KLRG1, MB21D1, DEFA4, TRIM32, LCK, DEFA3, SLPI, NAIP, CD300LB, CD244, HMGB2, FGR, JCHAIN, MAP4K2, TRDC, IRAK4, SERINC5, REL, IGHV3-23, IGHA1, ZAP70, IGHA2, FCER1G, CLEC6A, MR1, IGKC, PTX3, CD6, TRAF3, ITK, CR1, TRIM28, BMX, ANXA1,
GO:0042742:defense response to bacterium	IGHG1, IGHG2, IGHG3, IGHG4, S100A8, TLR1, S100A9, HP, TLR4, TRDC, TLR5, IL10, RAB1A, NLRC4, NOD2, CLEC4E, IGHV3-23, FCER1G, CLEC4D, IGKC, SPN, SYK, CEBPB, CEBPE, CAMP, ELANE, LYZ, ANXA3, S100A12, PLAC8, DEFA3, MPO, RBPJ, IGLC2, IGLC3
GO:0002755:MyD88-dependent toll-like receptor signaling pathway	IRAK4, IRAK3, LY96, MAP3K1, TLR1, TLR2, TLR4, TLR5, TLR7, RPS27A, TLR8, BTK
GO:0002223:stimulatory C-type lectin receptor signaling pathway	NFKBIA, NFKB1, RPS6KA5, CARD11, NRAS, PSMC6, PSMB6, PSMD12, PSMA6, CLEC4E, PSMD10, PSMB3, PSMD1, PSMC1, FCER1G, CLEC6A, CLEC4D, PSMD5, PSMD6, PSMD7, FBXW11, CHUK, RPS27A, SYK
GO:0002250:adaptive immune response	GPR183, CD244, CD8B, JCHAIN, IGHM, SKAP1, BTK, SH2D1A, CD46, FCGR1B, LILRA6, ZAP70, ERAP1, CD4, CLEC6A, CLEC4D, CD6, PAG1, SYK, ITK, DBNL, LAIR1, CRTAM, ADGRE1, SIT1, THEMIS, ANXA1, CD1C, EOMES, TNFRSF17, TRAT1, CTSL, LAT2, BTN3A1, CD86, CAMK4,
GO:0050853:B cell receptor signaling pathway	MEF2C, IGHG1, IGHG2, IGHG3, IGHG4, TRDC, IGHM, BTK, KLHL6, BCL2, IGHV3-23, ZAP70, IGHA1, IGHA2, IGKC, NFATC2, SYK, PTPRC, NCKAP1L, CD38, LAT2, LCK, IGLC2, IGLC3, PLEKHA1
GO:0050852:T cell receptor signaling pathway	CD247, NFKBIA, PTPN22, NFKB1, SKAP1, PTEN, TRAC, PSMB6, PSMB3, PDE4B, PSMD1, ZAP70, PIK3CA, CD4, PSMD5, PSMD6, PSMD7, FBXW11, CHUK, RPS27A, PAG1, CD28, ITK, PTPRC, CD3G, CD3D, THEMIS, PDE4D, TRBC1, TRAT1, CARD11, BTN3A1, PSMC6, PSMA6, PLCG1,
GO:0050871:positive regulation of B cell activation	IGHG1, IGHG2, IGHG3, IGHG4, TRDC, IGHM, NOD2, IGHV3-23, IGHA1, IGHA2, IGKC, TNIP2, IGLC2, IGLC3
GO:0031295:T cell costimulation	CD3G, CD3D, LGALS1, CD247, TRBC1, CDC42, CARD11, CD86, TRAC, TNFSF13B, ICOS, LCK, MAP3K8, PIK3CA, CD4, MAP3K14, CD5, DPP4, SPN, CD28
GO:0042110:T cell activation	ITK, CD3G, CD8A, CD8B, AZI2, HSH2D, CD86, NLRC3, NEDD4, RAB29, ZAP70, CD2, IRF4, DPP4
GO:0030217:T cell differentiation	PTPRC, PKNOX1, CD3D, PTPN2, LCK, ZAP70, PTPN22, CD4, KIT, IL7R, RUNX2
GO:0006955:immune response	AQP9, CD8A, IGHV3-48, CD8B, IGKV1-17, TLR1, TLR2, TLR4, HLA-DMB, VIPR1, HLA-DMA, TLR7, IL10, CD96, LTB4R, COL4A3BP, S1PR4, IL4R, CEACAM8, IL1RAP, SPN, CHUK, CIITA, IGLV1-51, IL18RAP, GZMA, TRBC1, CD164, GZMH, OSM, TNFRSF9, CD86, IGKV1-5, TNFSF13B, CST7, LAX1, IGLV7-43, SLPI, IGKV4-1, MAP3K14, PTGDR2, CTSG, IL1R2, GPR183, IGHV1-2, TNFRSF25, ENPP2, CYSLTR2, CCR1, JCHAIN, GPR65, MAP4K2, IL32, IL7R, CD74, IL10RB, ICOS, FCGR1A, FCGR1B, IGHV3-23, CNR2, IGHA1, ZAP70, IGHA2, CD4, MR1, IGKC, THBS1, CD27, IL18R1,
GO:0050776:regulation of immune response	IFITM1, CD8A, CD8B, IGHV3-48, IGKV1-17, CD247, SIGLEC9, CD96, SH2D1A, TRAC, FCGR1A, ITGB7, OSCAR, IGHV3-23, CLEC2D, IGKC, KLRB1, LAIR1, CRTAM, IGLV1-51, CD3G, CD3D, SELL, ICAM5, CD1C, CD160, NECTIN2, SPPL2A, ITGA4, TRBC1, IGHV3-30, CARD11, IGKV1-5, IGHV3-7, IGHV4-39, IGHV3-33, IGLV7-43, CD300LF, IGKV4-1, IGKV3-20, IGLC2, CD300LB, IGLC3, CD300LD
GO:0007249:I-kappaB kinase/NF-kappaB signaling	ROCK1, HACD3, LY96, TBK1, TIFA, NFKB1, TLR4, BIRC3, AZI2, TANK, TLR8, BTK, NLRC3, REL, RIPK3, MAP3K14, TNIP2, RPS27A, CHUK
GO:0006954:inflammatory response	PTGS2, S100A8, TBK1, S100A9, TLR1, TLR2, TLR4, NFKB1, TLR5, TLR7, IL10, TLR8, S1PR3, NLRC4, CXCR4, LTB4R, CXCR6, IL1RAP, VNN1, TNIP2, CHUK, SYK, CIITA, PTGER2, HYAL3, SP100, IL18RAP, LY96, LYZ, TNFRSF9, PROK2, ALOX15, KLRG1, CAMK4, CCR3, NAIP, NMI, TNFRSF25, FFAR3, CCR1, FPR1, KIT, FPR2, AZU1, REL, IL10RB, CNR2, ZAP70, PTX3, THBS1, CD27, CEBPB, OLR1, HCK, CHI3L1, ANXA1, PLGRKT, S100A12,
GO:0050900:leukocyte migration	CD244, MMP9, FPR1, FPR2, ITGAM, CD74, CD44, CD177, PDE4B, CEACAM8, CD2, CEACAM6, PIK3CA, FCER1G, CEACAM1, SPN, OLR1, ROCK1, SELL, ELANE, ITGA4, SLC16A3, NRAS, PLCG1, CD58, LCK, MERTK
GO:0000502:proteasome complex	RAD23B, KIAA0368, UBR1, PSMC6, PSMB6, PSMD12, VCP, PSMA6, PSMD10, PSMB3, PSMD1, PSMC1, PSMD5, PSMD6, PSMD7
GO:0004175:endopeptidase activity	TRABD2A, MMP9, APH1B, ELANE, MME, SENP2, PSMB6, PSMA6, PARL, TMEM59, CD46, PSMD1, ERAP1, HTRA3, ADAMTS3

Table 13 List of genes in each GO term resulted significantly enriched in the overrepresentation analysis.

Gene Ontology	Genes
GO:0070062:extracellular exosome	LDHB, LDHA, RPL14, RP2, PGD, IGHM, CTNNB1, OSCAR, VNN1, CAB39, DDAH2, GNG5, ADAM9, RAB27A, GLTP, RETN, RPS18, IGKV1-5, MGAM, RYR2, ARL8A, ARL8B, ZNHIT6, ADAMTS3, OSTF1, AHCY, GNAI3, DAAM2, HADHB, ARG1, FGL2, UBASH3A, RPS20, IGKC, RPSA, PTGR1, TAOK1, UPB1, UBE2L3, RPS5, RPS8, SYNE2, PI3, MCPH1, PCNA, TGFBR3, H3F3B, GK, DPP3, MARCKSL1, MTHFD1, MSRA, SMPDL3A, CEACAM8, DPP7, CEACAM1, DPP4, STX3, ELANE, TTC38, SDK1, LYZ, NECTIN2, ERLIN2, CLIC1, FLNB, NAPRT, CARD11, GNAQ, GNB2, TXN, SERPINB1, ALPL, SORD, JCHAIN, ABI1, ITM2C, ITM2A, NUMA1, UEVLD, PPP2CA, TBC1D4, ACSL4, VTA1, RPL26, TRIM23, TMEM2, PLSCR1, NRAS, IGHV3-7, RPL23, RPL22, GNG10, HIST1H2AH, SPG11, IGLC2, HPGD, CMTM6, ORM2, DNM2, SRP14, ATP6AP1, CAPZA2, CAPZA1, KIAA1324, SNRPD2, IQGAP1, PRKAR2A, FAM49B, SLC2A5, DDX23, SLC2A3, RALB, RNF149, ZNF445, RPS27A, NCALD, PATJ, PCOLCE2, ARPC1A, ARPC1B, FGR, ARPC4, ARPC5, ARPC3, ARPC2, RPL3, HIST1H4E, RPL5, RPL4, RPL10A, B4GALT5, RAB8B, FIBP, SPPL2A, RPL23A, MYL12B, MYL12A, LAMP1, LYVE1, VCP, PTTG1IP, HDHD2, HIST1H3F, CYB5R1, IMPA1, FIGNL1, IGKV1-17, HP, PRDX3, SYNGR2, HLA-DMA, RPS3, SLC1A4, CDC42, SNTB2, CDK5RAP2, RHOG, IMPDH2, SIT1, SPINT1, STXBP3, RPS4X, NCOA3, LCK, CA4, SNX12, UGP2, LCP1, GALNT3, CD101, GALNT2, SNX18, FKBP5, VIM, GALNT4, BTN2A2, CDH6, IARS, ALDH1A1, ZBTB8OS, ATIC, LRG1, TOR1A, HSPA6, TOR1B, HSPA7, VPS35, PLP2, TMC8, PDCD10, SLC12A2, OLR1, RNASE3, KL, ANXA1, GYG1, ANXA5, MAN1C1, FBL, ANXA3, AKR1B1, APAF1, GCA, VPS25, CADM4, S100A8, IL6ST, FAM20A, RAB3GAP1, S100A9, PPCS, GGT1, CD53, RAB1A, DNASE1L1, GOT2, CD44, DDX11, IFT20, CD46, RAB29, LILRA5, ERAP1, F12, DBNL, C1GALT1C1, SLC12A9, SUCLG1, DCTN2, PGM2, C1QB, CD38, RAB18, CAMK4, ALOX15B, TACSTD2, TXNDC5, VSIG4, TPST2, MME, EPHB4, CD74, CDC37, EPHB1, SERINC5, STX12, SERINC1, IGHV3-23, IDH2, ZMPSTE24, ST6GAL1, LAMTOR3, LGALS1, CHI3L1, NCKAP1L, LGALS8, CD63, PPA2, CD55, IGHV3-33, CD59, CD58, SLC46A3, PLAU, IGHG1, IGHG2, IGHG3, IGHG4, MYO7B, FERMT3, ACTR3, ACTR2, DNAJC13, CAP1, RAB6A, DOCK10, FAM129A, KCNMA1, CAMP, FLOT1, ATP6V1C1, EEF1A1P5, RAB5A, MTAP, SLC27A2, YWHAZ, FUT8, PRTN3, TFG, HPRT1, AZU1, IL10RB, CD177, PCMT1, THBS1, QSOX1, CD27, RAB2A, PSMD12, PYGL, MAPK14, ATP6V1E1, CAPG, IGKV3-20, FCGR2A, PGK1, TSPO, CHMP4C, NIT2, MMP9, NANS, TIAM2, PDGFC, SPN, NQO2, CUTA, IGLV1-51, MFGE8, LYPLA1, BASP1, PPP1CB, GNS, LAT2, PSMA6, DEFA3, CPD, SLC38A1, SEPT7, MVP, MYL6, SRI, WNT5B, ITGB4, NEDD8, NAPB, SNX3, LMAN2, LMAN1, ITGAM, CHMP2B, PEF1, GALM, PSMB6, ITGB7, PSMB3, BLOC1S1, GALC,
GO:0006888:ER to Golgi vesicle-mediated transport	COPA, DYNC1LI2, ARFGAP3, SEC24A, VAPA, ATL3, DYNC2LI1, LMAN2, LMAN1, RAB1A, COPB2, DDHD2, COPB1, RAB29, TGFA, SEC22B, SEC22C, SAR1B, RAB2A, SEC23A, DCTN6, VTI1A, BCAP31, DCTN2, COPG2, CD55, VCP, TRAPPC8, CD59, CNIH4, KLHL12, GOSR2, SEC23B
GO:0048208:COPII vesicle coating	SEC23A, PPP6C, SEC24A, TFG, PPP6R3, LMAN1, RAB1A, TRAPPC6A, SCFD1, ANKRD28, CD59, TRAPPC6B, TGFA, KLHL12, SEC22B, GOSR2, SAR1B
GO:0072562:blood microparticle	IGHG1, IGHG2, YWHAZ, IGHG3, IGHG4, IGKV1-17, JCHAIN, HP, HSPA1B, TRDC, IGHM, IGHV3-23, IGHA1, HSPA6, IGHA2, HSPA7, IGKC, CLIC1, DNPEP, STOM, C1QB, IGKV1-5, IGKV4-1, IGKV3-20, IGLC2, ORM2, IGLC3
GO:0006614:SRP-dependent cotranslational protein targeting to membrane	RPL18, SRP14, RPL19, RPL14, RPL35, RPS3, RPL6, RPL3, RPL5, RPL4, RPL10A, RPS20, RPS23, RPS27A, RPSA, SRP54, RPL26, RPL23A, SRPRB, RPS4X, RPS6, RPS5, RPS8, RPS18, RPL23, RPL18A, RPL13A, RPL22
GO:0006364:rRNA processing	RPL18, RNASEL, RPL19, RPL14, RPL35, NOB1, BMS1, RPS3, ISG20, WDR75, IMP3, RPL6, RPL3, RPL5, RPL4, RPL10A, RPS20, RPS27A, RPS23, NOL6, RPSA, EXOSC4, RPL26, RPL23A, LAS1L, HEATR1, DIEXF, DIS3L, RPS4X, RPS6, RPS5, FBL, RPS8, RPS18, RPL18A, RPL23, RPL22,
GO:0015935:small ribosomal subunit	RPSA, RPS18, IMP3, MRPS6, RPS20, RPS4X, RPS6, RPS5, RPS27A, RPS23, RPS3
GO:0022625:cytosolic large ribosomal subunit	RPL18, RPL19, RPL14, COA1, RPL26, RPL35, RPL23A, RPL23, RPL18A, RPL6, RPL13A, RPL22, RPL3, RPL5, RPL4, RPL10A
GO:0006413:translational initiation	RPL18, EIF4E3, RPL19, RPL14, RPL35, RPS3, RPL6, RPL3, EIF3L, RPL5, RPL4, RPS20, RPL10A, RPS23, RPS27A, ABCE1, RPSA, RPL26, RPL23A, RPS4X, RPS6, RPS5, RPS8, RPS18, RPL23, RPL18A, RPL13A, RPL22
GO:0003735:structural constituent of ribosome	RPL18, MRPS33, RPL19, RPL14, COA1, RPL35, MRPS31, MRPS30, RPS3, SLC25A20, IMP3, SLC25A24, RPL6, RPL3, SLC25A28, RPL5, RPL4, RPL10A, RPS20, SLC25A40, RPS23, RPS27A, RPSA, MRPS25, RPL26, RPL23A, MRPS6, RPS4X, RPS6, RPS5, RPS8, SLC25A11, RPS18,

Table 14 List of genes in each GO term resulted significantly enriched in the overrepresentation analysis.

9 SCIENTIFIC PRODUCTS

- Li M, Li Y, Weeks O, et al, “SOS2 and ACP1 Loci Identified through Large-Scale Exome Chip Analysis Regulate Kidney Development and Function”. J Am Soc Nephrol. 2016 Dec 5 [Epub ahead of print]
- F. Rizzi, C. Conti, E. Dogliotti, A. Terranegra, E. Salvi, D. Braga, F. Ricca, S. Lupoli, A. Mingione, F. Pivari, C. Brasacchio, M. Barcella, M. Chittani, F. D’Avila, M. Turiel, M. Lazzaroni, L. Soldati, D. Cusi, and C. Barlassina, “Interaction between polyphenols intake and PON1 gene variants on markers of cardiovascular disease: a nutrigenetic observational study.,” J. Transl. Med., vol. 14, no. 1, p. 186, 2016.
- F. D’Avila, M. Meregalli, S. Lupoli, M. Barcella, A. Orro, F. De Santis, C. Sitzia, A. Farini, P. D’Ursi, S. Erratico, R. Cristofani, L. Milanesi, D. Braga, D. Cusi, A. Poletti, C. Barlassina, and Y. Torrente, “Exome sequencing identifies variants in two genes encoding the LIM-proteins NRAP and FHL1 in an Italian patient with BAG3 myofibrillar myopathy,” Journal of Muscle Research and Cell Motility, pp. 1–15, 2016.
- N. Barizzone, I. Zara, M. Sorosina, S. Lupoli, E. Porcu, M. Pitzalis, M. Zoledziewska, F. Esposito, M. Leone, A. Mulas, E. Cocco, P. Ferrigno, F. R. Guerini, P. Brambilla, G. Farina, R. Murru, F. Deidda, S. Sanna, A. Loi, C. Barlassina, D. Vecchio, A. Zauli, F. Clarelli, D. Braga, F. Poddie, R. Cantello, V. Martinelli, G. Comi, J. Frau, L. Lorefice, M. Pugliatti, G. Rosati, M. Melis, M. G. Marrosu, D. Cusi, F. Cucca, F. Martinelli Boneschi, S. Sanna, and S. D’Alfonso, “The burden of multiple sclerosis variants in continental Italians and Sardinians.,” Mult. Scler., vol. 21, no. 11, pp. 1385–95, 2015.

- M. Chittani, R. Zaninello, C. Lanzani, F. Frau, M. F. Ortu, E. Salvi, G. Fresu, L. Citterio, D. Braga, D. a. Piras, S. D. Carpini, D. Velayutham, M. Simonini, G. Argiolas, S. Pozzoli, C. Troffa, V. Glorioso, K. K. Kontula, T. P. Hiltunen, K. M. Donner, S. T. Turner, E. Boerwinkle, A. B. Chapman, S. Padmanabhan, A. F. Dominiczak, O. Melander, J. a. Johnson, R. M. Cooper-Dehoff, Y. Gong, N. V. Rivera, G. Condorelli, B. Trimarco, P. Manunta, D. Cusi, N. Glorioso, and C. Barlassina, "TET2 and CSMD1 genes affect SBP response to hydrochlorothiazide in never-treated essential hypertensives," J. Hypertens., p. 1, 2015.
- J. Knez, E. Salvi, V. Tikhonoff, K. Stolarz-Skrzypek, A. Ryabikov, L. Thijs, D. Braga, M. Kloch-Badelek, S. Malyutina, E. Casiglia, D. Czarnecka, K. Kawecka-Jaszcz, D. Cusi, T. Nawrot, J. A. Staessen, and T. Kuznetsova, "Left ventricular diastolic function associated with common genetic variation in ATP12A in a general population.," BMC Med. Genet., vol. 15, p. 121, 2014.
- F. Frau, R. Zaninello, E. Salvi, M. F. Ortu, D. Braga, D. Velayutham, G. Argiolas, G. Fresu, C. Troffa, E. Bulla, P. Bulla, S. Pitzoi, D. A. Piras, V. Glorioso, M. Chittani, G. Bernini, M. Bardini, F. Fallo, L. Malatino, B. Stancanelli, G. Regolisti, C. Ferri, G. Desideri, G. A. Scioli, F. Galletti, A. Sciacqua, F. Perticone, E. Degli Esposti, A. Sturani, A. Semplicini, F. Veglio, P. Mulatero, T. A. Williams, C. Lanzani, T. P. Hiltunen, K. Kontula, E. Boerwinkle, S. T. Turner, P. Manunta, C. Barlassina, D. Cusi, and N. Glorioso, "Genome-wide association study identifies CAMKID variants involved in blood pressure response to losartan: The SOPHIA study," Pharmacogenomics, vol. 15, no. 13, pp. 1643–1652, 2014.
- E. Salvi, T. Kuznetsova, L. Thijs, S. Lupoli, K. Stolarz-Skrzypek, F. D'Avila, V. Tikhonoff, S. De Astis, M. Barcella, J. Seidlerova, P. Benaglio, S. Malyutina, F. Frau, D. Velayutham, R. Benfante, L.

Zagato, A. Title, D. Braga, D. Marek, K. Kawecka-Jaszcz, E. Casiglia, J. Filipovsky, Y. Nikitin, C. Rivolta, P. Manunta, J. S. Beckmann, C. Barlassina, D. Cusi, and J. A. Staessen, “Target sequencing, cell experiments, and a population study establish endothelial nitric oxide synthase (eNOS) gene as hypertension susceptibility gene,” Hypertension, vol. 62, no. 5, pp. 844–852, 2013.

- E. Salvi, Z. Kutalik, N. Glorioso, P. Benaglio, F. Frau, T. Kuznetsova, H. Arima, C. Hoggart, J. Tichet, Y. P. Nikitin, C. Conti, J. Seidlerova, V. Tikhonoff, K. Stolarz-Skrzypek, T. Johnson, N. Devos, L. Zagato, S. Guarrera, R. Zaninello, A. Calabria, B. Stancanelli, C. Troffa, L. Thijs, F. Rizzi, G. Simonova, S. Lupoli, G. Argiolas, D. Braga, M. C. D’Alessio, M. F. Ortu, F. Ricceri, M. Mercurio, P. Descombes, M. Marconi, J. Chalmers, S. Harrap, J. Filipovsky, M. Bochud, L. Iacoviello, J. Ellis, A. V. Stanton, M. Laan, S. Padmanabhan, A. F. Dominiczak, N. J. Samani, O. Melander, X. Jeunemaitre, P. Manunta, A. Shabo, P. Vineis, F. P. Cappuccio, M. J. Caulfield, G. Matullo, C. Rivolta, P. B. Munroe, C. Barlassina, J. A. Staessen, J. S. Beckmann, and D. Cusi, “Genomewide association study using a high-density single nucleotide polymorphism array and case-control design identifies a novel essential hypertension susceptibility locus in the promoter region of endothelial NO synthase,” Hypertension, vol. 59, no. 2, pp. 248–255, 2012.

10 ACKNOWLEDGMENTS

I would like to thank the Doctorate school of Molecular and Translational Medicine for the opportunity to do my PhD and for funding me over the three years.

I express my gratitude to my tutor Cristina Barlassina for guiding me in the research work and for the constant support and availability.

I am grateful to Matteo Barcella for the friendly help during my work

I would like to thank all the colleagues I worked with during these three years. In particular I thank Francesca D'Avila and Federico Tagliaferri.

I would like to thank Simon Moxon and Earlham Institute for the opportunity to learn about the analysis of microRNA sequencing data.

I'm grateful to all the people in the Shockomics Consortium

Finally I sincerely thank my family